

# TULAMEEN RIVER COANDA SCREEN WEIR DESIGN FOR THE TOWN OF PRINCETON, BC

Department of Civil Engineering  
British Columbia Institute of Technology  
Burnaby, BC



*(Knight Piesold Consulting, 2021)*

**Prepared for:** \_\_\_\_\_, Industry Project Sponsor  
Industry Projects Committee, BCIT Civil Engineering Department  
Phyllis Chong, P.Eng, Project Coordinator, BCIT  
Jan Bielenberg, P.Eng, Faculty Advisor, BCIT  
Jacquie Russell, BA, Communication Instructor, BCIT

**Prepared by:** \_\_\_\_\_ (A#####)

**Submitted on:** MM DD, YYYY

## DISCLAIMER

This report is intended for educational purposes and created by engineering students at the British Columbia Institute of Technology. All work and analysis performed is purely academic in nature and based upon (in-part) fictitious information. No part of this report may be copied or referenced for estimating, construction, analysis, or other professional purposes of any kind. Readers engaging in unauthorized use shall accept full liability for the application of information used from this report.

## ACKNOWLEDGEMENTS

I would like to thank the following people who helped me devise and research this project:

- Jan Bielenberg, who was always there to answer my questions and provided professional feedback on hydraulics and provided direction in site location and flood analysis
- \_\_\_\_\_, who advised on the development and research papers on Coanda screen design
- \_\_\_\_\_, who offered paternal advice, provided sketches and made recommendations on foundation design
- \_\_\_\_\_, whose experience in dam construction lent well to understanding the hydraulic forces on the weir structure

MM DD, YYYY

\_\_\_\_\_  
P.Eng.  
Industry Project Sponsor

\_\_\_\_\_  
\_\_\_\_\_, \_\_\_\_\_

Dear \_\_\_\_\_

### **Submission of Final Report: Tulameen River Coanda Screen Weir Design**

Please find enclosed my report on the design of a weir structure utilizing Coanda screens for the Town of Princeton. The project focused on a run-of-the-river design on the Tulameen River with the purpose of providing hydraulic head to a hypothetical hydro-electric station.

The content of this report discusses how the river discharges were calculated and the weir structure was designed. Within the report, you will find details on the Coanda Effect and how an optimal screen was chosen for this application. After more than 150 hours of research, drafting, calculations and correspondence dedicated to this project over the course of the last 4 months, I was able to finalize a possible design solution.

Although much more research could have been undertaken in this review, I feel this was a good first-attempt at researching and developing hydraulic concepts within the scope and allotted time. The knowledge and experience gained from this project will certainly aid me in future studies and in composing formal reports.

I want to express my appreciation in your willingness to sponsor and review my report. I am also thankful for your providing the reference information on Coanda screen design. That information proved invaluable in assisting me with the design and in ultimately accomplishing this project.

If you have any questions regarding the attached report, I can be reached at (xxx) xxx-xxxx or \_\_\_\_\_ . I look forward to hearing from you.

Sincerely,

\_\_\_\_\_

cc: Jan Bielenberg, Faculty Advisor  
Jacquie Russell, Communication Instructor

Attachment: final report

## SUMMARY

The purpose of this report was to research and design a run-of-the-river weir structure for the Town of Princeton, British Columbia.

Although the scenario is fictitious in nature, the project was based on a situation that could one day be at the forefront of a small town's proposal for a bid on a design. The purpose of this project was to assess the viability of a weir structure for the generation of hydro-electric power and thus increase the delivery of green energy for a burgeoning industrial and residential population.

\_\_\_\_\_, my industry sponsor, supported the concept behind this project and believes it to be a good exercise in academic research.

My project was limited to the study of the weir design structure and did not include additional research into the hydro-electric facility.

River analysis was undertaken using data taken from Gauge Station 08NL024 near Princeton and a potential site location for the weir structure was located. Using Manning's Equation and local topography, the river's cross sections, discharge rates and varying depths were all evaluated.

Using the Gumbel Method, a 100-year return was extrapolated and a maximum peak discharge of  $650 \text{ m}^3/\text{s}$  was calculated. This predicted value was then used to design the height of the wing walls of the weir structure.

The Standard Step Method was used to calculate the backwater profile curve and to determine an acceptable distance of gradually varied flow. This information was then used to design the height of the backwall of the structure. An overall concrete structure was then drafted with Autodesk software using these input parameters.

Based on the average discharge rate of the river, the Ogee Spillway formula was used to optimize the weir's width, calculated at approximately 70m.

A soil mechanics analysis was performed on the midspan of the structure to determine the factor of safety against uplift forces and overturning moments. Both factors of safety were deemed acceptable based on the quantity and configuration of concrete used.

The Coanda screen design for this project was based largely in part from experimental data taken from the United States Department of the Interior. Based on the calculated average river discharge, an Ogee crest was designed along with an accelerator drop plate and optimal Coanda screen configuration (length, tilt, curvature, etc.).

Based on the relative topography of the area, a tentative location for a powerhouse was selected and an ideal power output was calculated. The results of that output classify this structure as meeting a mini-station qualification.

All relevant calculations, drawings and schematics have been included in the body of the report or in an appropriate appendix as required.

Further considerations for this project would be additional research into sediment control, studying the effects of a 200-year return flood on the weir structure and exploring ways to increase the potential power output.

## TABLE OF CONTENTS

|     |  |    |
|-----|--|----|
| 1.0 | INTRODUCTION .....                               | 1  |
| 1.1 | Background on Coanda Screens.....                | 2  |
| 1.2 | Site Description .....                           | 2  |
| 2.0 | RIVER FLOW ANALYSIS AND WEIR DESIGN.....         | 3  |
| 2.1 | Background .....                                 | 3  |
| 2.2 | Weir Location.....                               | 7  |
| 2.3 | Design of Weir Channel.....                      | 8  |
| 2.4 | Tulameen River Flood Analysis at Princeton ..... | 11 |
| 2.5 | Gumbel Method.....                               | 13 |
| 2.6 | Soil Mechanics .....                             | 16 |
| 2.7 | Specific Energy .....                            | 18 |
| 2.8 | Energy Dissipation .....                         | 22 |
| 2.9 | Sediment Control & Maintenance.....              | 23 |
| 3.0 | COANDA SCREENS.....                              | 23 |
| 3.1 | Background .....                                 | 25 |
| 3.2 | Debris Control.....                              | 26 |
| 3.3 | Design Parameters.....                           | 30 |
| 3.4 | Screen Capacity Theory .....                     | 30 |
| 3.5 | Implementation & Calculations .....              | 30 |
| 3.6 | Designing the Ogee Curve .....                   | 31 |
| 3.7 | Concrete Structure.....                          | 38 |
| 3.8 | Unit Discharge and Hydropower.....               | 40 |
| 4.0 | CONCLUSION.....                                  | 42 |
| 5.0 | RECOMMENDATIONS & DISCUSSION .....               | 43 |
| 5.1 | Comparison to Traditional Hydro .....            | 44 |
| 5.2 | River Flood Analysis.....                        | 45 |
|     | REFERENCES .....                                 | 46 |
|     | APPENDICES .....                                 | 47 |
|     | Appendix A: Fish Bypass .....                    | 47 |
|     | Appendix B: Gauge Station .....                  | 48 |
|     | Appendix C: Tulameen Discharge & Depth.....      | 49 |
|     | Appendix D: Manning Coefficients.....            | 50 |

|   |    |
|---|----|
| Appendix E: Trapezoidal Channel Calculations..... | 51 |
| Appendix F: Trapezoidal Section at Site .....     | 52 |
| Appendix G: Yearly Peak Flow Data .....           | 53 |
| Appendix H: The Standard Step Method.....         | 54 |
| Appendix I: The Gumbel Method.....                | 55 |
| Procedure .....                                   | 55 |
| Appendix J: Soil Mechanics Calculations .....     | 57 |
| Simpson’s Method.....                             | 58 |
| Concrete Weight & Factor of Safety.....           | 58 |
| Overturning Moment.....                           | 59 |
| Appendix K: Ogee Profile .....                    | 61 |
| Appendix L: Concrete Weir Structure .....         | 62 |

## LIST OF ILLUSTRATIONS

### FIGURES

|  |    |
|--|----|
| Figure 1 Site Location .....   | 3  |
| Figure 2 Gauge Station 08NL024 on the Tulameen River .....                     | 4  |
| Figure 3 Trapezoidal section with geometric variables .....                    | 5  |
| Figure 4 Slope of the Tulameen River.....                                      | 6  |
| Figure 5 Proposed weir location .....  | 7  |
| Figure 6 Peak discharge (red) and mean discharge (green).....                  | 8  |
| Figure 7 Freeboard calculation for a 2m high weir.....                         | 9  |
| Figure 8 Backwater profile extent.....   | 10 |
| Figure 9 Kettle Valley Rail Bridge .....                                       | 11 |
| Figure 10 Peak annual discharge rates over a 40-year period .....              | 12 |
| Figure 11 Peak instantaneous discharge .....                                   | 13 |
| Figure 12 Extrapolated discharge rates.....                                    | 14 |
| Figure 13 Floodplain based on a 200-year rain event.....                       | 15 |
| Figure 14 Soil strata in the Tulameen area .....                               | 16 |
| Figure 15 Flow net under a weir structure .....                                | 16 |
| Figure 16 Flow net under proposed weir structure .....                         | 17 |
| Figure 17 Predicted depth of flow up and downstream of the weir structure..... | 18 |
| Figure 18 Specific energy diagram .....  | 19 |
| Figure 19 Hydraulic Jump .....   | 21 |

|  |    |
|--|----|
| Figure 20 Stilling basin.....                                    | 22 |
| Figure 21 Aqua Shear Intake Screen profile by Aquadyne Inc. .... | 24 |
| Figure 22 Experimental test of Coanda screens.....               | 25 |
| Figure 23 A typical Coanda-screen illustration .....             | 26 |
| Figure 24 Wedge-wire profile.....                                | 26 |
| Figure 25 Slot openings of the wedge-wire screen.....            | 27 |
| Figure 26 Oriented slope of the screens.....                     | 27 |
| Figure 27 Wedge-wire tilt from horizontal.....                   | 28 |
| Figure 28 The effect of tilting wires on orifice flow .....      | 28 |
| Figure 29 Collection chamber.....                                | 29 |
| Figure 30 Accelerator plate drop height .....                    | 29 |
| Figure 31 Flow profile over a weir spillway.....                 | 31 |
| Figure 32 Ogee Profile.....                                      | 32 |
| Figure 33 Ogee compound curve trajectory.....                    | 33 |
| Figure 34 Optimal Coanda profile .....                           | 34 |
| Figure 35 Discharge vs. Drop Height .....                        | 35 |
| Figure 36 Unit Discharge vs. Accel. Drop.....                    | 36 |
| Figure 37 Unit Discharge vs. Screen length .....                 | 37 |
| Figure 38 Unit Discharge vs. Screen slope.....                   | 38 |
| Figure 39 Proposed concrete structure.....                       | 39 |
| Figure 40 Overhead view of the weir structure .....              | 39 |
| Figure 41 Another view of the structure .....                    | 40 |
| Figure 42 Powerhouse schematic.....                              | 40 |
| Figure 43 Tentative location for powerhouse .....                | 41 |
| Figure 44 Weir with stilling basin .....                         | 44 |
| Figure 45 Fish bypass .....                                      | 47 |
| Figure 46 Depth & Discharge.....                                 | 49 |
| Figure 47 Open channels .....                                    | 51 |
| Figure 48 Flow net and uplifting forces.....                     | 57 |
| Figure 49 Overturning moments.....                               | 59 |
| Figure 50 Calculated Ogee profile.....                           | 61 |
| Figure 51 Concrete Weir Structure.....                           | 62 |

## TABLES

|   |    |
|---|----|
| Table 1 Discharge and depth at gauge station .....                              | 4  |
| Table 2 Typical Values of Manning's n .....                                     | 7  |
| Table 3 Upstream normal depth calculation for a trapezoidal cross section ..... | 10 |
| Table 4 Results of the Gumbel Method .....                                      | 14 |
| Table 5 River channel depth calculation.....                                    | 20 |

|   |    |
|---|----|
| Table 6 Standard Step Method results .....                      | 21 |
| Table 7 Ogee curve data .....                                   | 32 |
| Table 8 Ogee curve coordinates.....                             | 34 |
| Table 9 Classification of run-of-the-river stations.....        | 42 |
| Table 10 Gauge Station.....                                     | 48 |
| Table 11 Roughness coefficients .....                           | 50 |
| Table 12 Calculations of existing channel section.....          | 51 |
| Table 13 Normal flow depth.....                                 | 52 |
| Table 14 Peak annual discharge.....                             | 53 |
| Table 15 Output from the Standard Step Method.....              | 54 |
| Table 16 Frequency Factors for Gumbel Method.....               | 55 |
| Table 17 Frequency and Probability .....                        | 56 |
| Table 18 Calculations detailing the resultant uplift force..... | 58 |

## 1.0 INTRODUCTION

For my project, I am proposing to implement a Coanda screen weir structure on the Tulameen River in Princeton, B.C. for the purpose of hydro-electric power generation.

My project is sponsored by \_\_\_\_\_, of \_\_\_\_\_. \_\_\_\_\_ believes that this project will be a very informative approach to develop my knowledge of hydrological principles and their applicability towards hydraulic design. He will provide guidance to ensure that the hydraulic concepts of this proposal are consistent and relevant.



*(Knight Piesold Consulting, 2021)*

The objectives of this project are to:

- Select an appropriate site along the river for the weir
- Determine the optimal Coanda screen configuration for this application
- Analyze how upstream flow will be affected by the weir installation
- Estimate a reasonable power output based on flow to the penstock
- Describe qualitatively and mathematically the physics of Coanda screens in regard to flow-rate
- Discuss any concerns about erosion control and hydraulic stability

The construction details of the hydro-plant and the required earthworks are beyond the scope and will therefore not be included in this project. Environmental impacts will be limited to upstream and downstream water level changes. Fish first design is also beyond the scope of this report; however, the author does acknowledge that Coanda screens allow for fish migration (Appendix A: Fish Bypass).

The site description will be discussed in the background section. The following sections of this proposal will describe the Coanda screen and river flow analysis, and also provide some

recommendations. All pertinent calculations and schematics will be included in an appendices section along with a conclusion that looks at the overall picture and feasibility.

The information found in Section 3.2 on Coanda Screen Debris Control is all taken from (Douglass) and includes all explanations and graphics.

## 1.1 Background on Coanda Screens

Coanda Screens are a new, low profile improvisation to shallow weirs, which offer a unique solution to debris handling and improvement in water flow. Conventional designs require mechanized maintenance for debris removal and additional structures such as fish ladders, and do not optimize water intake. Coanda screens have been shown to eliminate operational costs of erosion damage, function at low temperatures and are aquatic life friendly (Mefford, 2013). For these reasons, Coanda screens are becoming increasingly popular and are the preferred method of weir design on run-of-the-river applications.

In this exercise, the Town of Princeton is looking for alternative ways to deliver green energy to its residents and local industry. This proposal is part of the Town's green initiative, promoting new and advanced sources of renewable energy for its local industry and residents. A Coanda screen weir design was decided to be the most suitable approach to distribute green energy to Princeton's residents.

## 1.2 Site Description

With the Tulameen River forming a confluence with the Similkameen River to the town's East, a site was chosen upstream on the Tulameen River. This location is suitable to develop a small hydro station due to cadastral availability and ease of access via a service road.

The selected site is about 2.1 kilometers upstream of The Brown Bridge along Bridge Street and can be accessed along a public works road. At the site of the proposed location, the river is 25 metres in width at low discharge, and averages about 0.667 metres in depth. Figure 1 shows an aerial view of the town with a red box indicating the site location.



Figure 1 Site Location (in red) (Regional District of Okanagan - Similkameen, 2021)

## 2.0 RIVER FLOW ANALYSIS AND WEIR DESIGN

### 2.1 Background

The government of Canada provides real-time and historical data for the Tulameen River. The data for this project was acquired from a gauge station that provides discharge rates and depths of flows. This data was examined over a span of years and also during a specifically chosen year.

This data was then used as a foundation for all subsequent calculations and designs of the weir structure.

Analysis began by locating the gauge station along the Tulameen River at Princeton. The station, 08NL024, is located at coordinates: Lat: 49° 27' 27" N, Long. 120° 31' 06" W and is shown below in Figure 2. For more information on the station, refer to Appendix B: Gauge Station.



Figure 2 Gauge Station 08NL024 on the Tulameen River (Regional District of Okanagan - Similkameen, 2021)

The proposed weir location is upstream of this gauge station, but due to its relative proximity, data taken from the gauge station can be assumed to be valid for the river discharge at the site location.

Low-level aerial photography and contour mapping was consulted to determine the relative cross section of the Tulameen River at 08NL024. The cross section is best approximated by a symmetrical trapezoidal section. To further refine the geometry, Manning's Equation (1) was implemented with the assistance of spreadsheet software (MS Excel) to determine the roughness coefficient of the riverbed.

Manning's Equation is given by:

$$Q = \frac{A}{n} * R^{\frac{2}{3}} * \sqrt{S} \quad (1)$$

where,

$Q = \text{discharge rate (m}^3/\text{s)}$

$A = \text{Cross sectional area (m}^2\text{)}$

$S = \text{hydraulic gradient (m/m)}$

$R = \text{Hydraulic Radius (m)}$

$n = \text{roughness coefficient}$

Now, with two given discharge rates and corresponding river depths as shown in Table 1, the geometry of the cross section was calculated.

Table 1 Discharge and depth at gauge station

| Discharge (m <sup>3</sup> /s) | Depth (m) | Month     | Year |
|-------------------------------|-----------|-----------|------|
| 4.32                          | 0.448     | August    | 2018 |
| 3.52                          | 0.410     | September | 2018 |

These values were taken from the Government of Canada website for 2018 and are displayed in Appendix C: Tulameen Discharge & Depth. The year 2018 was chosen arbitrarily.

Equation (1) was applied for the two data sets, and rearranged so that:

$$\frac{Q1}{Q2} = \frac{A1}{A2} * \left(\frac{R1}{R2}\right)^{2/3}$$

and using MS Excel's iterative solver, a value for  $m$  of 33.5 was determined and the top width of the channel,  $T$ , calculated to be about 35m.

This value for  $m$  is a very shallow side slope but realistic based on a flat bottom width,  $b$ , of 5m and the relatively low depth of water. Figure 3 illustrates a symmetric trapezoidal section and relevant geometric variables. Appendix E: Trapezoidal Channel Calculations details the output from the computations.

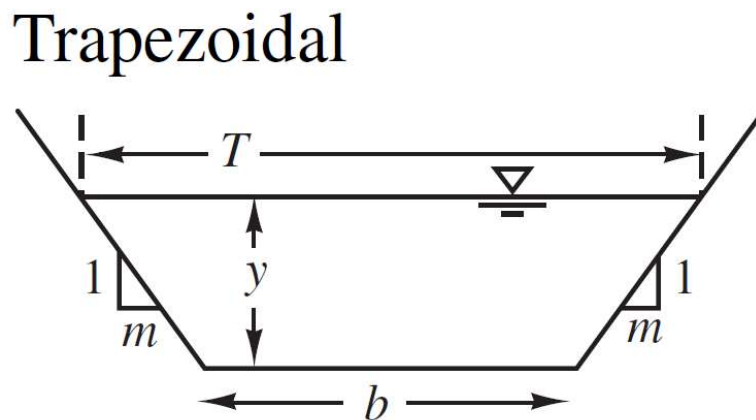


Figure 3 Trapezoidal section with geometric variables (Houghtalen, Akan, & Hwang, 2010)

The existing slope of the river in the vicinity was manually calculated from the graph shown below in Figure 4 with a value of 0.0033 or 0.33%. This data was taken from a topographic survey (Hay & Company Consultants Inc, 1995).

Although relatively steep compared to usual open channels and rivers, given the mountainous nature of the terrain, this value seemed reasonable. Equation 2 shows the slope calculation.

$$slope = \frac{rise}{run} = \frac{5.25m}{1600m} \times 100\% = 0.33\% \quad (2)$$

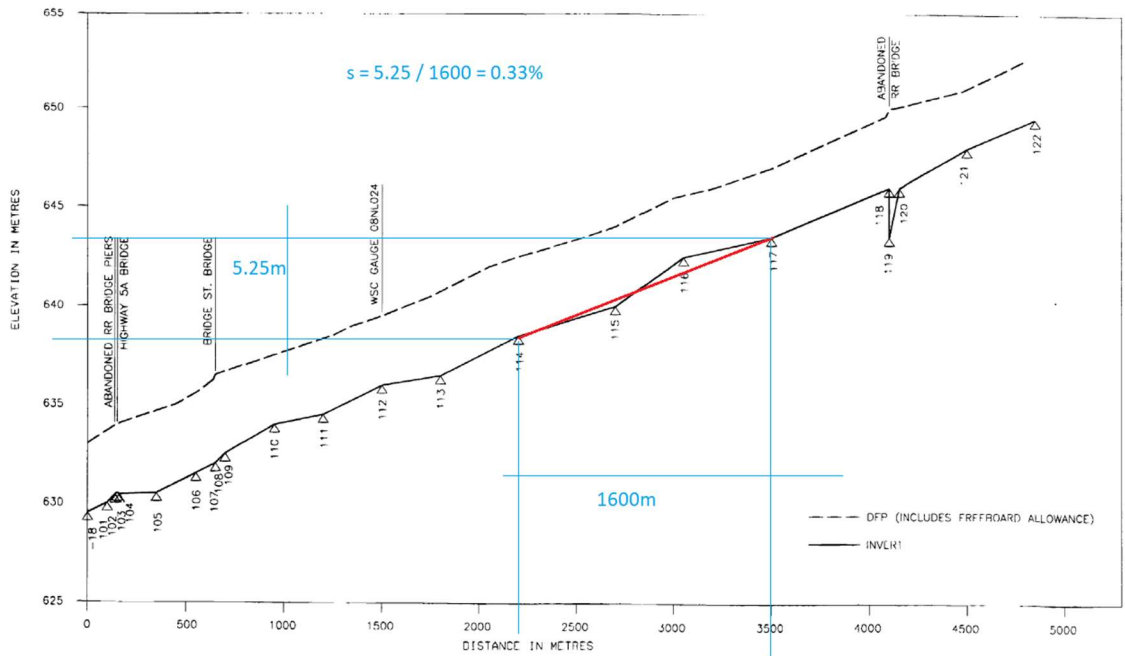


Figure 4 Slope of the Tulameen River (Hay & Company Consultants Inc, 1995)

With the geometry of the channel computed and verified from aerial photography (the top width of 35m is in good accordance with recent imaging), Equation (1) was further used to determine the roughness coefficient,  $n$ , of the riverbed.

By rearranging equation 1 such that

$$n = \frac{A}{Q} * R^{\frac{2}{3}} * \sqrt{S} = \frac{8.98}{4.32} * \left(\frac{8.98}{35.10}\right)^{\frac{2}{3}} * \sqrt{0.0033} = 0.048$$

this results in a roughness coefficient ( $n$  value) of 0.048.

Comparing this value to a standard table of values shown in Appendix D: Manning Coefficients, the value accords well with a mountain stream with gravel and cobbles as expected. Table 2 below is an excerpt from a list of roughness coefficients.

Table 2 Typical Values of Manning's  $n$  (Houghtalen, Akan, & Hwang, 2010)

| Channel Surface                             | $n$         |
|---|-------------|
| Riprap lined channel                        | 0.035-0.045 |
| Natural channels, clean and winding         | 0.035-0.045 |
| Natural channels, winding, pools, shoals    | 0.045-0.055 |
| Natural channels, weeds, debris, deep pools | 0.050-0.080 |
| Natural channels, gravel and cobbles        | 0.030-0.50  |
| Natural channels, cobbles and boulders      | 0.050-0.070 |

## 2.2 Weir Location

The design analysis for the weir began at the proposed site location and with the determination of the normal flow depth. This location is shown below in Figure 5 with coordinates:

Lat: 49° 27' 10" N, Long. 120° 32' 13" W

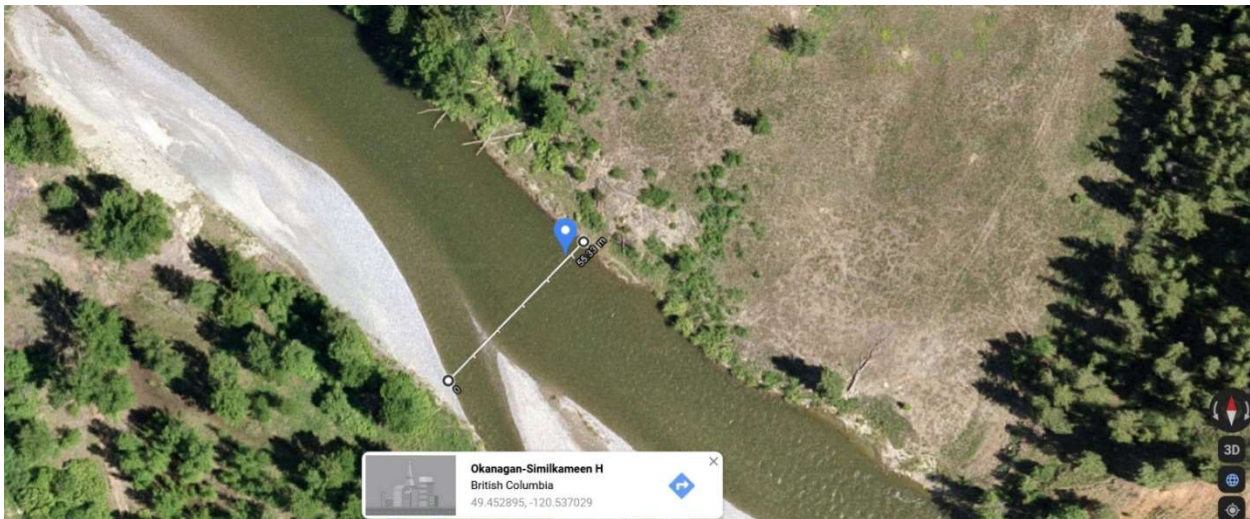


Figure 5 Proposed weir location (Regional District of Okanagan - Similkameen, 2021)

The average span (Top width,  $T$ ) of the channel at this location is approximately 55m and is based on an average discharge rate of 30.0  $\text{m}^3/\text{s}$  (cumecs). Figure 6 below shows the peak discharge throughout the year for 2018 and the rationale for choosing 30  $\text{m}^3/\text{s}$  as the average baseline discharge was intuited from the output.

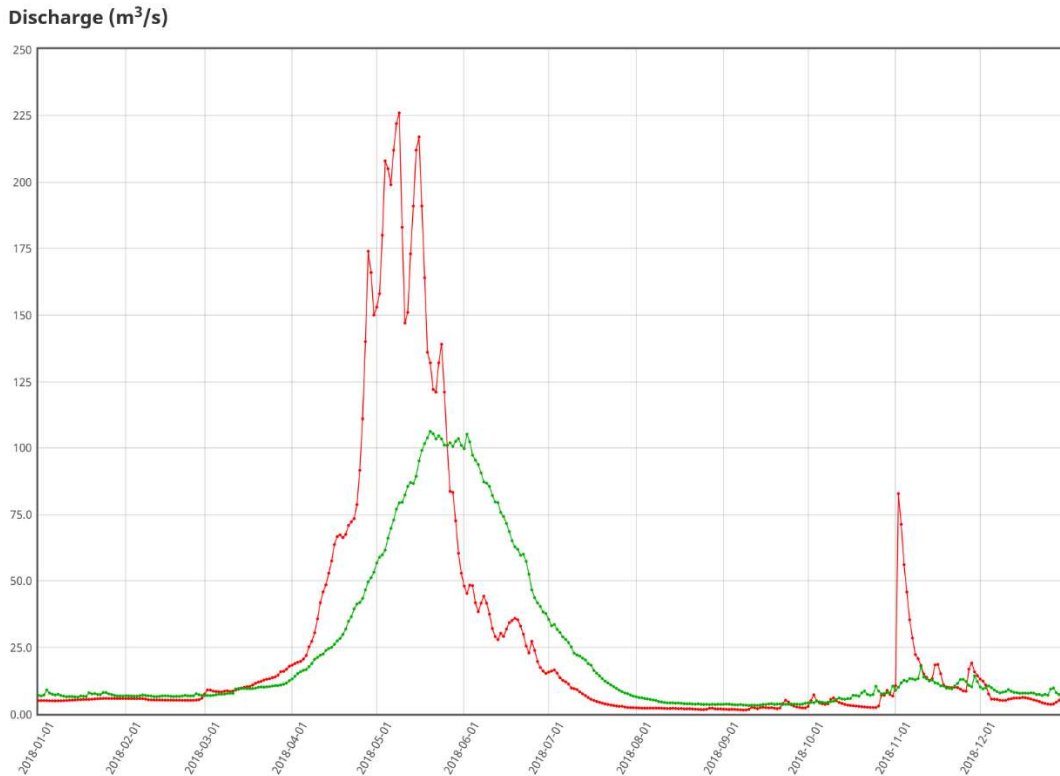


Figure 6 Peak discharge (red) and mean discharge (green) (Government of Canada, 2021)

Manning’s Equation (1) was then applied to determine normal flow conditions. The average discharge is taken from Station 08NL024 for the year of 2018 as mentioned previously.

The river cross section was determined to be an asymmetrical trapezoid as shown in Appendix F: Trapezoidal Section at Site and applied with geometric variables of  $m = 10$  and  $b = 25\text{m}$  based on the existing topography. Again, by using Equation (1) with an average discharge of  $30\text{m}^3/\text{s}$ , a flow depth of  $0.67\text{m}$  was iteratively calculated.

### 2.3 Design of Weir Channel

The channel was designed to accommodate a large flow up to 200 cumecs (based on peak monthly flows in Appendix G: Yearly Peak Flow Data) while still maintaining efficiency of water conveyance and safety. A weir span of 70m was chosen with a concrete-lined rectangular cross section and angled wing walls. This wider channel was chosen to minimize the backwater effects on the river depth.

An average annual flow of 30 cumecs was used to optimize the design height and, using the Ogee Spillway formula:

$$Q = C * L * H^{\frac{2}{3}} \quad (3)$$

where  $L$  is the length of the weir,  $H$  is the head over the weir crest, and  $C$ , the discharge coefficient is given by

$$C = 2/3^{3/2} * g^{1/2}$$

where  $g = 9.81 \text{ m/s}^2$  is the acceleration due to gravity.

A freeboard height,  $H$ , was calculated to be 0.4m for a 2.0m high weir as shown in Figure 7 below. Further information on this can be found in Section 3.0 on the Coanda screen design.

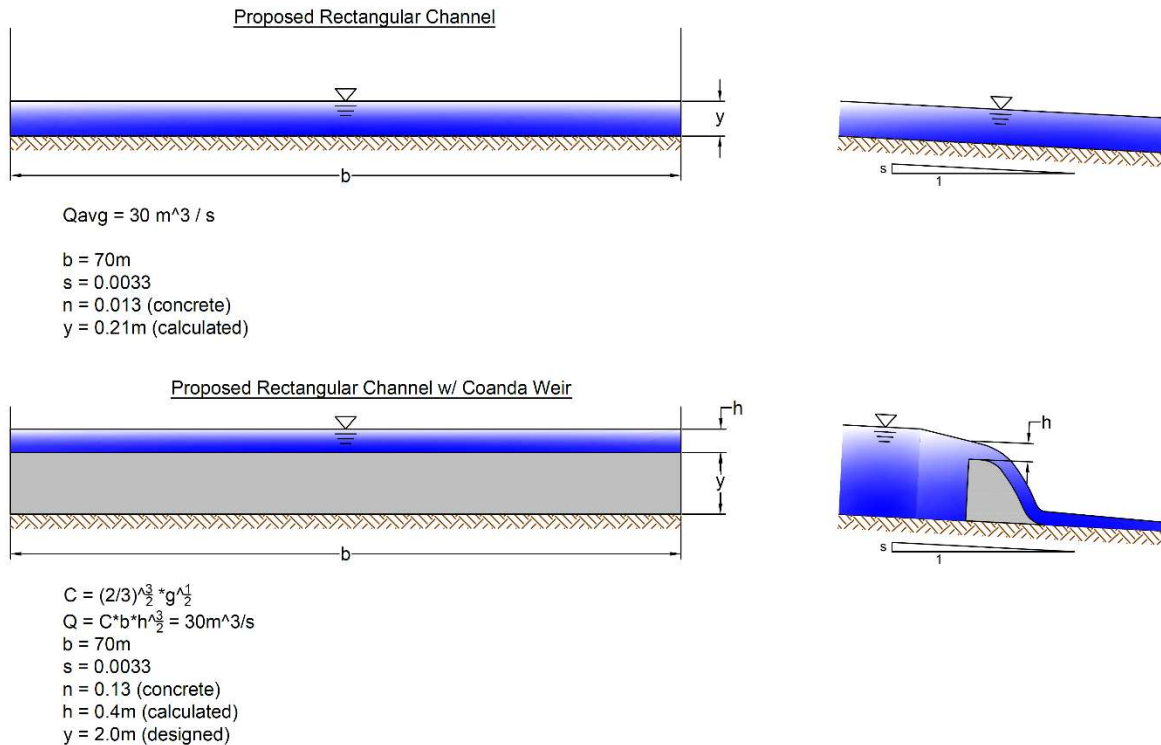


Figure 7 Freeboard calculation for a 2m high weir

Of importance was to determine the effects that the weir proposal would have on the backwater depth. Essentially a dam, the weir will raise the water level at the site and induce a sub-critical flow that will reach a steady-state equilibrium further upstream before returning to its normal flow depth (Houghtalen, Akan, & Hwang, 2010).

The Standard Step method was used to determine the reach of river that would be affected by the increase in river depth. Just upstream of the excavated channel, the structure will transition from having concrete wing walls (see Appendix L: Concrete Weir Structure) to a natural river channel, still at 70m in width and rectangular in cross section.

At this stage, the average river depth will be 2.4m in height and will gradually transition to a normal depth of 0.91m further upstream where the river will return to an average width of about

25m. These values were calculated using a combination of the Manning's and Ogee Spillway equations with the iterative solver. The output data is shown below in Table 3.

Table 3 Upstream normal depth calculation for a trapezoidal cross section

| River Channel Backwater to Normal Depth |        |                         |
|---|--------|-------------------------|
| <i>Trapezoid</i>                        |        |                         |
| <b>n =</b>                              | 0.048  | <i>calculated</i>       |
| <b>s<sub>0</sub> =</b>                  | 0.0033 | m/m                     |
| <b>b =</b>                              | 25.000 | m                       |
| <b>Q<sub>avg</sub> =</b>                | 30.000 | m <sup>3</sup> /s       |
| <b>normal depth</b>                     |        |                         |
| <b>y<sub>normal</sub> =</b>             | 0.914  | m ( <i>calculated</i> ) |
| <b>Area =</b>                           | 31.215 | m <sup>2</sup>          |
| <b>Pw =</b>                             | 43.376 | m                       |
| <b>Rh =</b>                             | 0.720  | m                       |
| <b>Target Q</b>                         | 30.000 | m <sup>3</sup> /s       |
| <b>Q<sub>avg</sub> =</b>                | 30.000 | m <sup>3</sup> /s       |

The Standard Step Method was then implemented to calculate the backwater distance. Appendix H: The Standard Step Method describes the method in some detail and lists the results. The distance was calculated as 474m and this stretch is approximately shown in Figure 8 below with changes in water depth.



Figure 8 Backwater profile extent

Upstream of the proposed weir location is an abandoned railway bridge (Kettle Valley Rail Bridge) which has since been repurposed to be used as part of a hiking trail. How the weir might affect the river depth near bridge was of due concern, but from the backwater profile calculations, it was determined not to be an issue as normal depth is re-established further downstream.



Figure 9 Kettle Valley Rail Bridge (Google Earth, 2021)

See the discussion section for more information on these changes and other considerations.

## 2.4 Tulameen River Flood Analysis at Princeton

The Tulameen River is subject to high and low discharges throughout the year and the weir design must be able to handle high-capacity discharges.

My advisor suggested that a 200-year return flood analysis be performed to check the effects of the maximum peak instantaneous discharge at this location on the river.

Data for flood analysis was taken from the Government of Canada's website. Gauge Station 08NL024 at Princeton has statistical data recorded from 1952 to the current date, but statistical values are available only until 2018. Instantaneous annual peak flow values recorded during this period are shown in Figure 10 in green for a 40-year period starting in 1974.

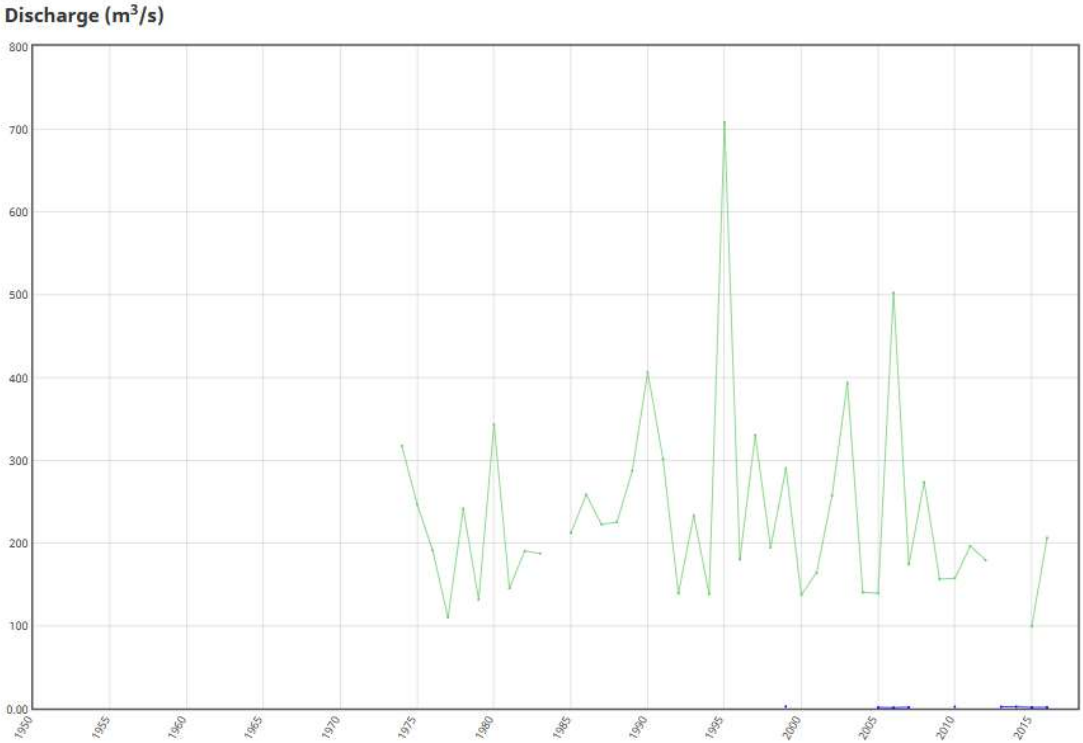


Figure 10 Peak annual discharge rates over a 40-year period (Government of Canada, 2021)

Peak flow values in red (2018) are also shown for comparative purposes in Figure 11. Values are taken based on a maximum daily discharge and plotted.

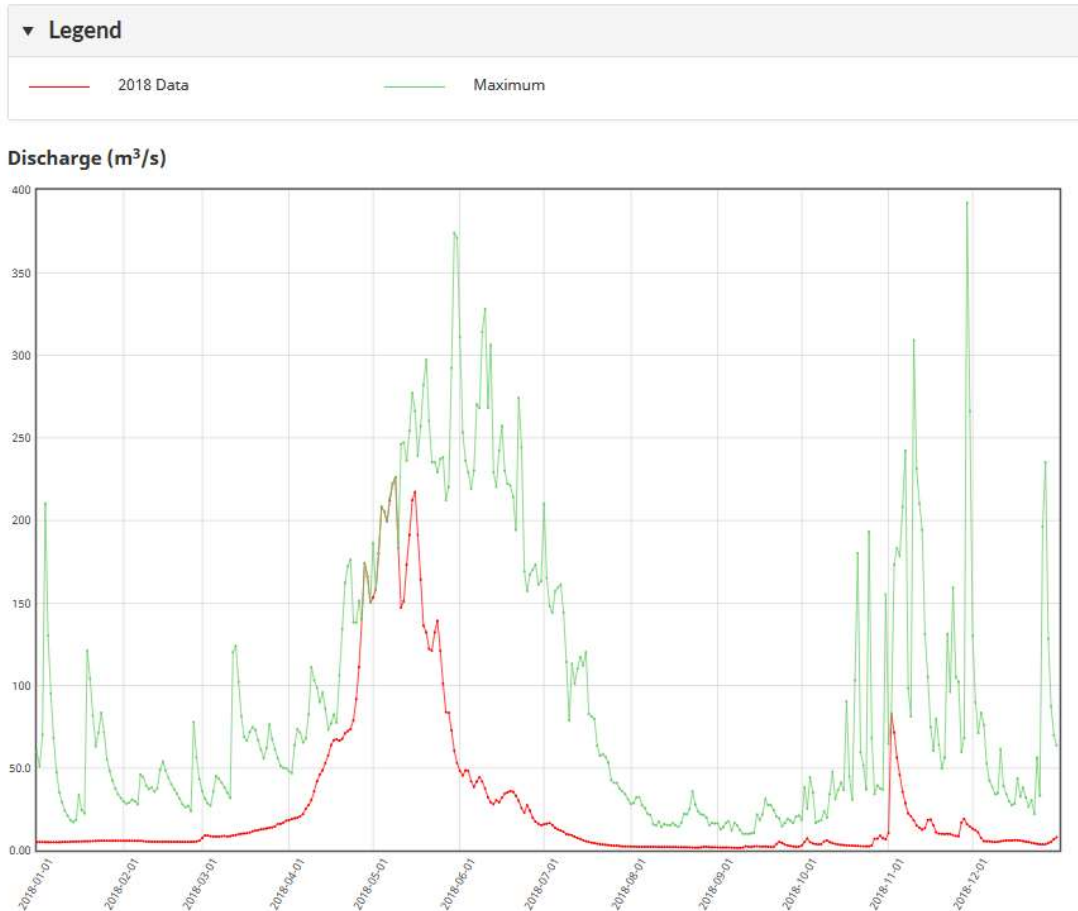


Figure 11 Peak instantaneous discharge (red) (Government of Canada, 2021)

Appendix I: The Gumbel Method shows the instantaneous peak discharge over a 40-year period, starting in 1974 and ending in 2016. Several years did not have available data and were disregarded. This data was used to extrapolate flood return periods using the Gumbel Method and a 100-year return was calculated.

## 2.5 Gumbel Method

The Gumbel Method was implemented to determine the maximum instantaneous peak flow for flooding. Data was collected based on the previous 40 years provided by the Government of Canada.

An instantaneous peak flow of approximately 650 m<sup>3</sup>/s was determined for a 100-year return storm as shown in Table 4 and Figure 12.

Table 4 Results of the Gumbel Method

| Return Period T (years) | x      | S      | K (Table XX) | KS     | Flood flow (cumecs) |
|-------------------------|--------|--------|--------------|--------|---------------------|
| 5                       | 234.91 | 114.80 | 0.84         | 96.20  | 331.11              |
| 10                      | 234.91 | 114.80 | 1.50         | 171.62 | 406.53              |
| 20                      | 234.91 | 114.80 | 2.13         | 244.06 | 478.97              |
| 50                      | 234.91 | 114.80 | 2.94         | 337.85 | 572.76              |
| 100                     | 234.91 | 114.80 | 3.55         | 407.99 | 642.90              |

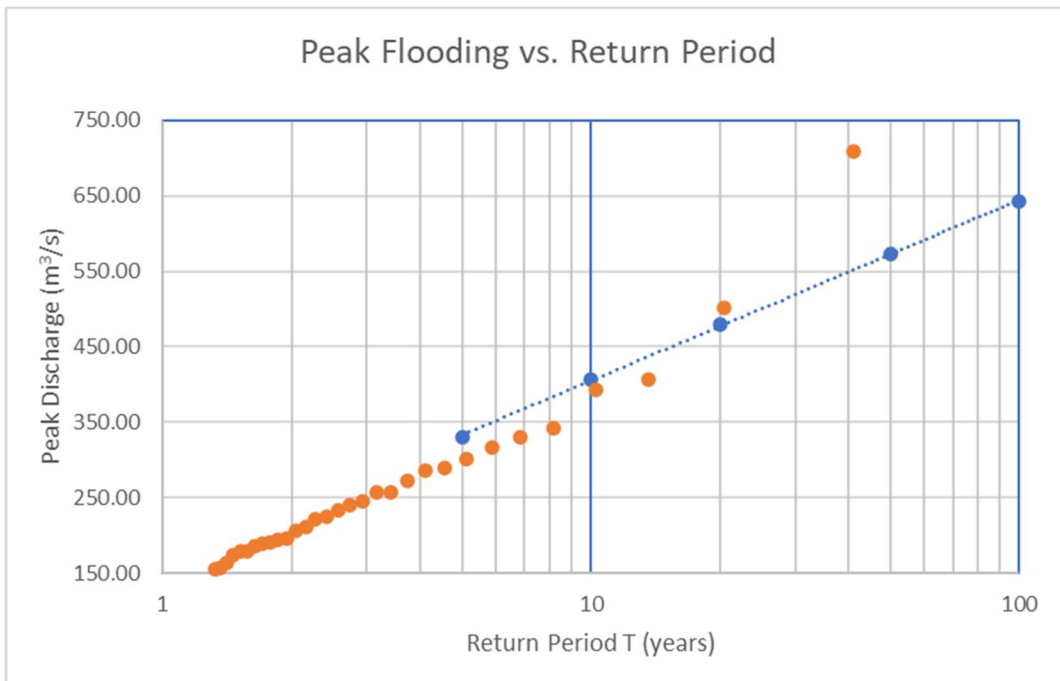
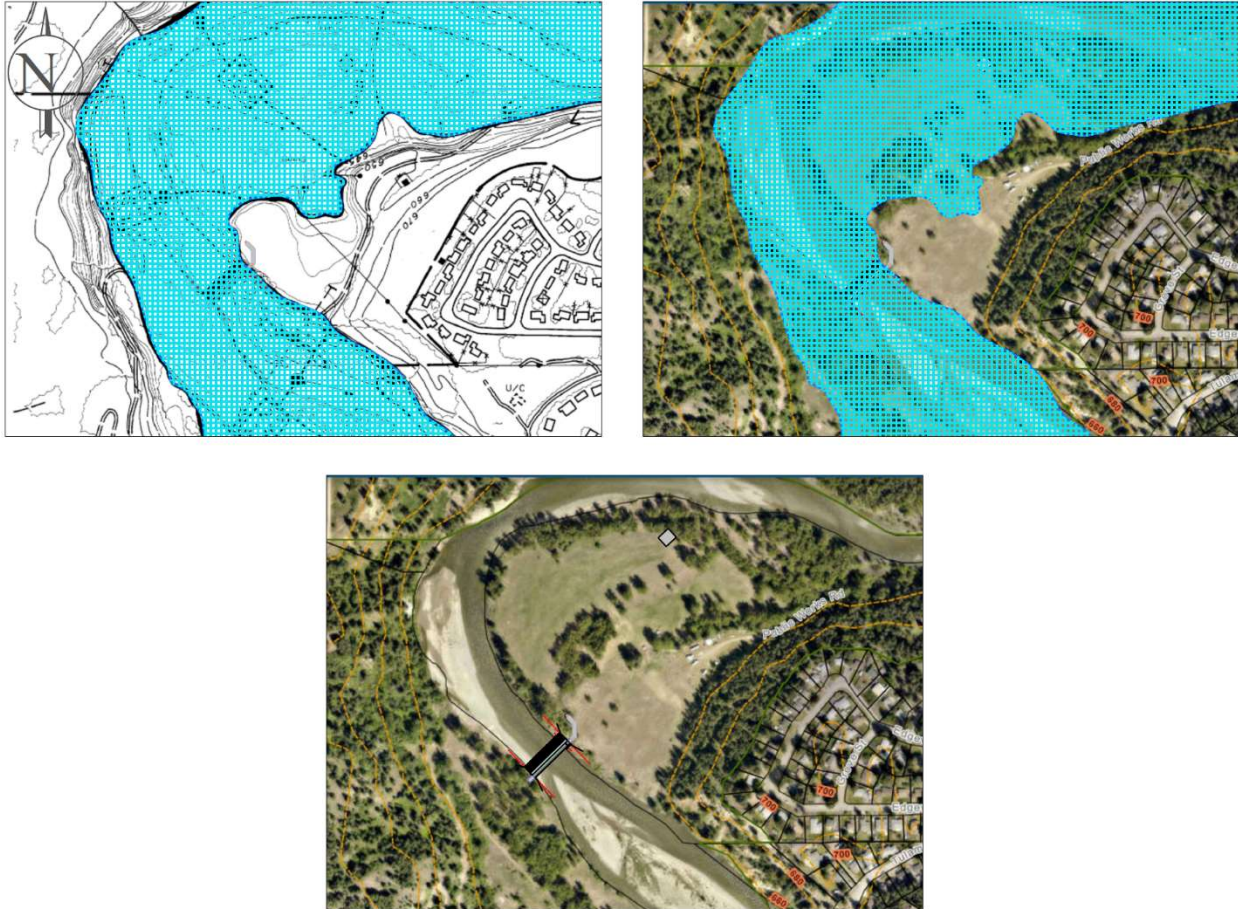


Figure 12 Extrapolated discharge rates

Looking at the topography of the area and the localized sections of the site location, an increase in river flow of 3m would result from a discharge of 650 m<sup>3</sup>/s. This rise in water level would submerge the weir structure and partially flood the up and downstream areas as shown in Figure 13.



*Figure 13 Floodplain based on a 200-year rain event*

One remedy to this is that the design of the wingwall height be set to a minimum of 5 meters as the increased peak discharge would submerge the weir spillway but the concrete structure would still contain the flow rate.

A study was conducted by (Hay & Company Consultants Inc, 1995) to investigate flooding of the Princeton area and included 5km along the Tulameen upstream of the confluence. The study concluded that the depth of river would increase by 4.0 meters based on a 200-year return event.

The effects of such flooding would need to be further evaluated by hydrological specialists in this field ultimately before a final decision on the weir proposal is made. See more on this in the recommendations section.

## 2.6 Soil Mechanics

The Tulameen riverbed has a layer of bedrock overlain with a till and morainal gravels. A soil study by (Lord & Green, 1974) investigated the Princeton area and soil depositions. Figure 14 shows a typical cross section of the soil strata in the area.

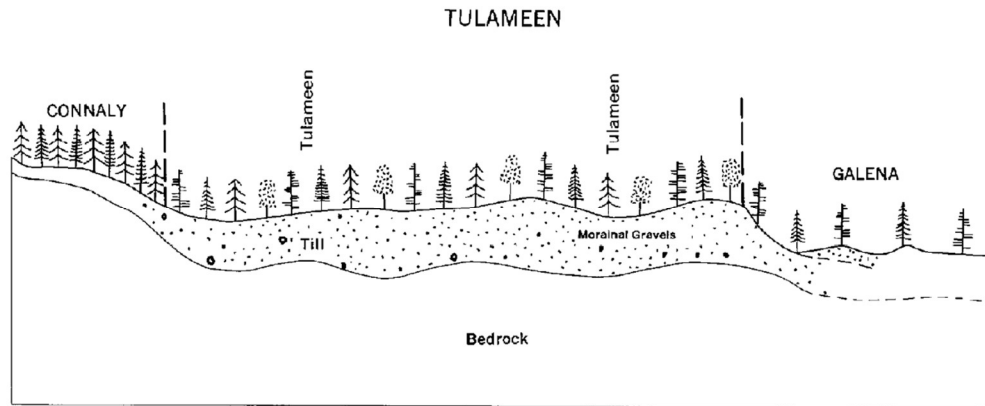


Figure 14 Soil strata in the Tulameen area (Lord & Green, 1974)

Under a weir structure, hydrostatic uplift forces may develop from the permeability of water and resulting seepage.

By approximating the seepage as two-dimensional flow and applying Laplace's Equation, the flow of water through the porous soil can be calculated. The Laplace equation describes the energy loss associated with the flow of water through a soil and is expressed as

$$k_x * \left(\frac{d^2h}{dx^2}\right) + k_y * \left(\frac{d^2h}{dy^2}\right) = 0 \quad (4)$$

with  $h$  being the energy potential or the total head and  $k_x$  and  $k_y$  are the permeability coefficients in the X and Y directions. See Figure 15 below.

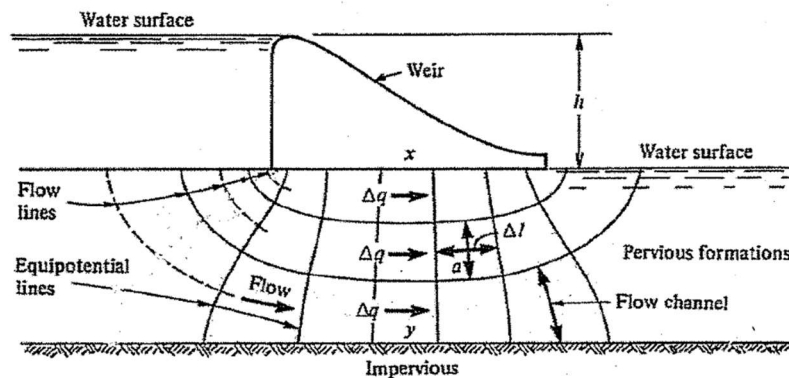


Figure 15 Flow net under a weir structure (Coduto, Yeung, & Kitch, 2011)

Assumptions made regarding these conditions:

- The voids are filled with water (100% saturation)
- The soil layer is homogenous and the coefficient of permeability is constant (glacial till everywhere above bedrock and k is uniform)
- The soil and water are incompressible
- The flow of ground water is laminar

With these assumptions, the equation can be simplified to

$$\left(\frac{d^2h}{dx^2}\right) + \left(\frac{d^2h}{dy^2}\right) = 0 \quad (5)$$

The solution to Equation 5 can be solved graphically through use of the flow net described in Appendix J: Soil Mechanics Calculations.

The flow net for the weir design is shown below in Figure 16. Due to a conservative approach of assuming a depth of up to 5.5 meters of till before the stratum of bedrock is reached, it is recommended that a sheet pile be installed. In this way, the uplift forces will be counteracted by the weight of the bulk concrete used and a factor of safety of 1.95 is achieved. Appendix J: Soil Mechanics Calculations details the calculations and also the safety factors against overturning.

These calculations are for the midspan of the structure away from the wingwalls where the mass of concrete is lowest and flow velocity would be largest.

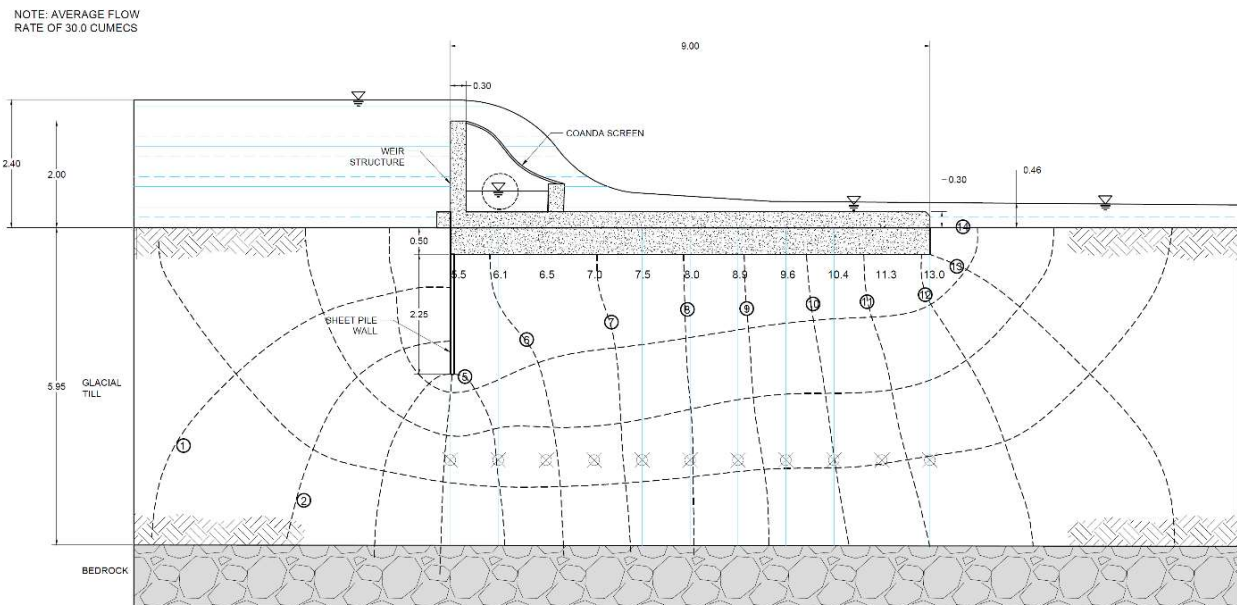


Figure 16 Flow net under proposed weir structure

## 2.7 Specific Energy

Specific energy is taken as the velocity head and the depth of flow in an open channel. Along with techniques from the standard step method, specific energy was used to analyze the flow depths in this stretch of the river. Its equation is given below.

$$E = \frac{v^2}{2 \cdot g} + y = \frac{Q^2}{2 \cdot g \cdot A^2} + y = \frac{Q^2}{2 \cdot g \cdot (b \cdot y)^2} + y \quad (6)$$

Referring to Figure 17 below, for a specific discharge,  $Q = 30 \text{ m}^3/\text{s}$  and a width  $b = 70\text{m}$ ,

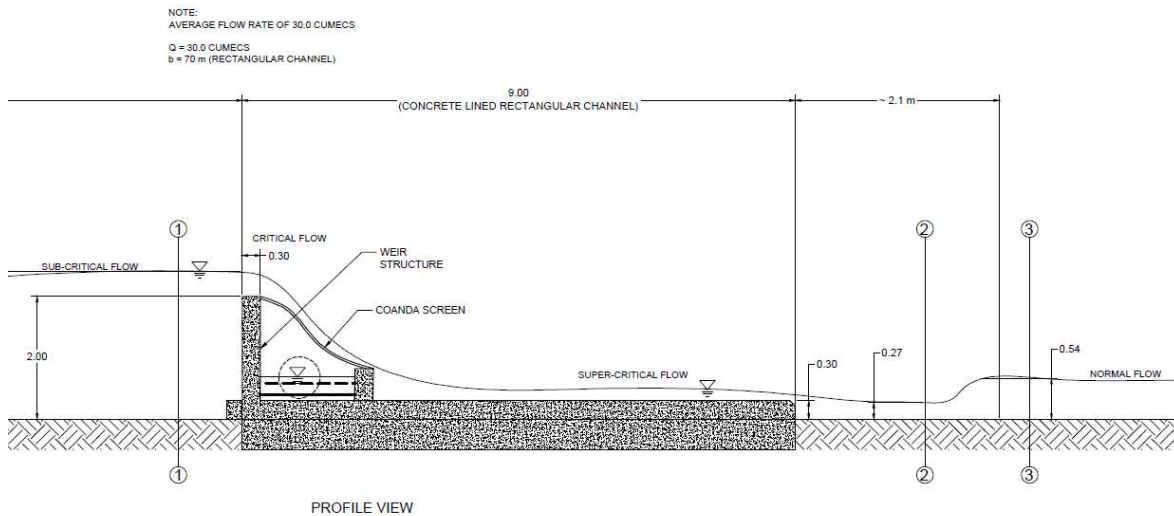


Figure 17 Predicted depth of flow up and downstream of the weir structure

at 1-1, the specific energy was calculated as,

$$E_1 = \frac{30^2}{2 \cdot 9.81 \cdot (70 \cdot 0.4)^2} + 2.4 = 2.46\text{m}$$

and this can be considered the normal energy in the channel.

Now, without loss of generality, at 2-2, assuming zero head loss between sections 1 and 2, the depth of flow can be iteratively computed using equation 6 for an unknown value of  $y$ . One expects a higher velocity at a shallower depth for a given energy and thus the value is computed as:

$$y = 0.063\text{m}$$

$$E_2 = 2.46\text{m} = \frac{Q^2}{2 \cdot g \cdot (b \cdot y)^2} + y = \frac{1}{107 \cdot y^2} + y \rightarrow y = 0.0625\text{m} \cong 0.063\text{m} \quad (7)$$

Over the spillway, there is a transition of the specific energy from subcritical flow to supercritical flow and thus, critical flow is achieved to minimize the energy required at the crest of the spillway.

This value was found directly as the vertex of the specific energy diagram by plotting  $y$  (flow) versus  $E$  (specific energy).

Substituting values into Equation 7, the below relation was plotted with Specific Energy ( $E$ ) as a function of  $y$  (flow depth). Conventionally,  $E$  is plotted on the horizontal axis as shown in Figure 18 below.

$$E = \frac{Q^2}{2 * g * (b * y)^2} + y = \frac{30^2}{2 * 9.81 * (70 * y)^2} + y = \frac{1}{107 * y^2} + y$$

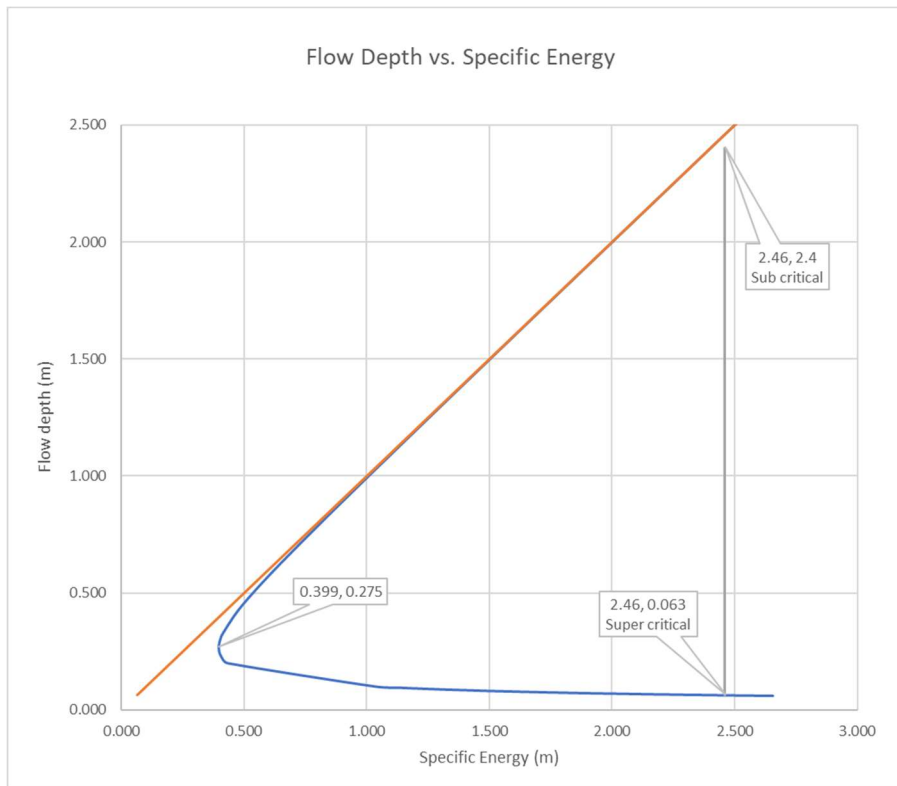


Figure 18 Specific energy diagram

As noted, the critical flow depth can be graphically inferred from the vertex of the semi-parabola. It appears to be close to 0.27m in depth.

Now, with the equation of the Froude number given by

$$N_F = \frac{v}{\sqrt{g*y}} , \text{ where } v = \frac{Q}{b*y} \quad (8)$$

and setting it equal to 1, it can be rearranged such that for a constant discharge and channel width the critical depth  $y$  is given by:

$$y_{critical} = \sqrt[3]{\frac{Q^2}{b^2 * g}} = 0.27\text{m}$$

Since the depth of flow at section 2 is supercritical and below the critical depth, a potential for a hydraulic jump may occur. In the rectangular excavated channel, it was determined that the normal depth of flow was found to be 0.54m using (1). See Table 5 below for the output of the calculations.

*Table 5 River channel depth calculation*

| <b>Proposed Rectangular Channel Section River lining<br/>Downstream</b> |        |                            |  |
|---|--------|----------------------------|--|
| <b>n =</b>  | 0.048  | river                      |  |
| <b>s =</b>  | 0.0033 |                            |  |
| <b>b =</b>  | 70.0   | m                          |  |
| <b>Q<sub>avg</sub> =</b>  | 30.00  | m <sup>3</sup> /s          |  |
| <b>Find depth, y =</b>  | 0.54   | m ( <i>Initial Guess</i> ) |  |
| <b>Area =</b>   | 38.03  | m <sup>2</sup>             |  |
| <b>Pw =</b>   | 71.09  | m                          |  |
| <b>Rh =</b>   | 0.54   | m                          |  |
| <b>Target Q</b>   | 30.00  | m <sup>3</sup> /s          |  |

From Figure 18, a depth of 0.54m corresponds to a specific energy of approximately the same amount (0.54m) since this is in the linear section of the graph.

Since this normal flow represents a drop in energy from section 2 having a specific energy of 2.46m, dissipation of this energy will occur downstream of the weir through a hydraulic jump.

The jump will raise the flow depth from  $y_1$  to  $y_2$ , the supercritical depth to the sequent depth. The sequent depth, shown as  $y_2$  in Figure 19 below,

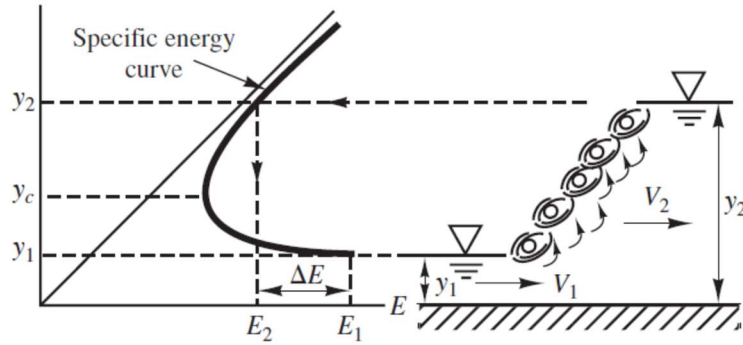


Figure 19 Hydraulic Jump (Houghtalen, Akan, & Hwang, 2010)

was found by first calculating the Froude number corresponding to  $y_1$  (in the supercritical regime).

$$N_{F1} = \frac{v}{\sqrt{g \cdot y}} = \frac{30 / ((70)(0.063))}{\sqrt{(9.81)(0.063)}} = 8.65 \text{ with } y_1 = 0.063\text{m}$$

The sequent depth, was then calculated with the below equation which only depends upon  $y_1$  and the Froude number.

$$y_2 = (y_1/2)(\sqrt{1 + 8(N_{F1})^2} - 1) \quad (9)$$

$$y_2 = \left(\frac{0.063}{2}\right)(\sqrt{1 + 8(8.65)^2} - 1) = 0.74\text{m}$$

This is a marginal increase in depth but nonetheless a water profile was used to determine the distance until this sequent depth was achieved at section 3.

Using the Standard Step Method, the transition from 0.063m in depth to 0.74m in flow depth was calculated to occur over a horizontal distance of 4.6 meters, an almost instantaneous transition. Table 6 shows the calculation output below.

Table 6 Standard Step Method results

| Section | Depth - y (m) | Area A (m <sup>2</sup> ) | Wetted Perimeter Pw | Hydraulic Radius R | Velocity | Energy | SI     | SAVG   | Delta L |
|---------|---------------|--------------------------|---------------------|--------------------|----------|--------|--------|--------|---------|
| 1       | 0.0630        | 4.4100                   | 70.1260             | 0.0629             | 6.8027   | 2.4217 | 2.9608 | 1.5885 | 4.2793  |
| 2       | 0.1382        | 9.6764                   | 70.2765             | 0.1377             | 3.1003   | 0.6281 | 0.2163 | 0.1336 | 0.1117  |
| 3       | 0.2135        | 14.9428                  | 70.4269             | 0.2122             | 2.0077   | 0.4189 | 0.0510 | 0.0348 | 0.0091  |
| 4       | 0.2887        | 20.2091                  | 70.5774             | 0.2863             | 1.4845   | 0.4010 | 0.0187 | 0.0087 | 0.0168  |
| 5       | 0.3639        | 25.4755                  | 70.7279             | 0.3602             | 1.1776   | 0.4346 | 0.0087 | 0.0066 | 0.0265  |
| 6       | 0.4392        | 30.7419                  | 70.8783             | 0.4337             | 0.9759   | 0.4877 | 0.0046 | 0.0037 | 0.0310  |
| 7       | 0.5144        | 36.0083                  | 71.0288             | 0.5070             | 0.8331   | 0.5498 | 0.0027 | 0.0017 | 0.0333  |
| 8       | 0.5896        | 41.2747                  | 71.1793             | 0.5799             | 0.7268   | 0.6166 | 0.0017 | 0.0015 | 0.0346  |
| 9       | 0.6649        | 46.5410                  | 71.3297             | 0.6525             | 0.6446   | 0.6860 | 0.0012 | 0.0010 | 0.0355  |
| 10      | 0.7401        | 51.8074                  | 71.4802             | 0.7248             | 0.5791   | 0.7572 | 0.0008 | 0.0010 | 0.0355  |
| sum =   |               |                          |                     |                    |          |        |        |        | 4.5777  |

Therefore, the channel downstream of the weir will not require extensive excavation to produce the 70m wide channel and can return to the natural 25m width with sloped sides.

## 2.8 Energy Dissipation

Downstream of the weir, it was recommended to include a stilling basin. This has the added effect of reducing the specific energy. By lowering the specific energy, soil erosion is mitigated. Figure 20 below shows a typical stilling basin of cobbles and boulders.



*Figure 20 Stilling basin (Knight Piesold Consulting, 2021)*

It is also worth calculating the change in Froude number from super critical flow to subcritical (sequent) flow after the hydraulic jump. Hydraulic jumps have the benefit of dissipating energy that flows over the spillway and further prevent possible erosion and scouring due to the high-water velocities (Houghtalen, Akan, & Hwang, 2010)

Equation (8) was used to calculate the Froude number in the supercritical regime and was determined as  $N_{F1} = 8.65$

In the subcritical (sequent depth) regime, the Froude number was calculated as  $N_{F2} = 0.21$  using Equation 8 and 9.

$$N_{F2} = \frac{v}{\sqrt{g * y_2}} = \frac{30/((70)(0.74))}{\sqrt{(9.81)(0.74)}} = 0.21$$

The below equation was then used to calculate the energy loss through the hydraulic jump.

$$\Delta E = E_1 - E_2 = \frac{(y_2 - y_1)^3}{4y_1y_2} = \frac{(0.74 - 0.063)^3}{4(0.74)(0.063)} = 1.66m \quad (10)$$

. This change represents a significant energy loss downstream of the weir which is ideal.

## 2.9 Sediment Control & Maintenance

Although the Coanda Screen is known to have low maintenance due to the self-cleaning aspects of its bypass flow, silt can build up behind the weir structure. As a result, it is recommended that a sluice gate be incorporated into the design midspan. The overall width of the Coanda Screens will remain at 70m but the design of an opening for the release of silt will be considered.

## 3.0 COANDA SCREENS

Traditional water technologies require the screening of incoming water to prevent small aquatic organisms and fine debris from accumulating at intakes. When finer screens are required to filter out smaller material, regular maintenance is incurred at higher costs regardless of water flow velocities.

With larger sized screen openings, less cleaning is required but at the trade-off of permitting larger debris to enter and contribute to clogging.

One screen design that offers efficiently screening of smaller particles with less clogging or required cleaning is the Coanda Screen (also referred to as Coanda-effect screen) shown below in Figure 21.

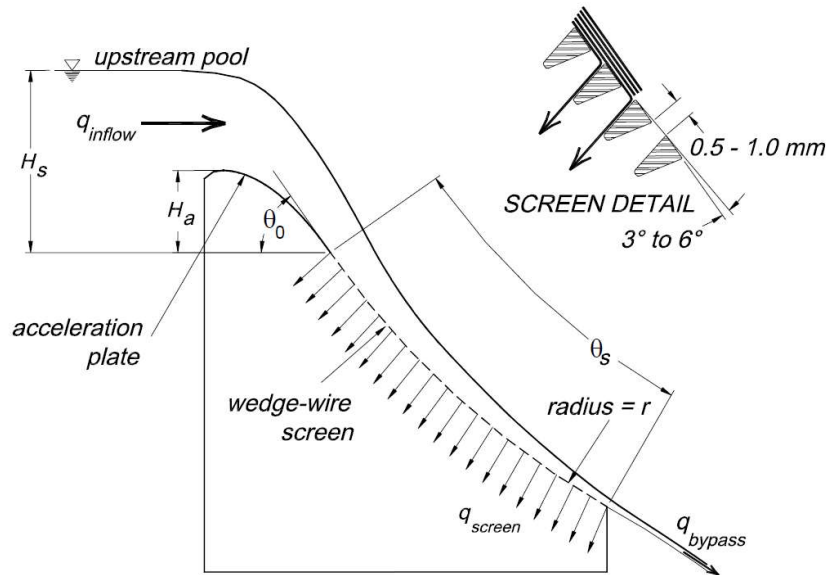


Figure 21 Aqua Shear Intake Screen profile by Aquadyne Inc. (Wahl, 2003)

This design has been incorporated in many run-of-the river projects in British Columbia, successfully reducing debris infiltration, saving maintenance costs and improving fish migration.

Screens are generally installed downstream of an overflow weir and that was the design adopted in this project with inflow capacities ranging from 0.09 – 0.14 m<sup>3</sup>/s per linear width of weir length (Wahl, 2003).

According to the U.S. Department of the Interior, researchers have “conducted extensive laboratory tests and developed a numerical model that can be used to predict Coanda-effect screen capacity and analyze the influence of design parameters. This testing included a prototype-size Coanda-effect screen structures (Figure 22) and small screen coupons tested in a special flume to determine the discharge coefficients of tilted-wire screen materials.”



Figure 22 Experimental test of Coanda screens (Wahl, 2003)

The department then used a computer program to model several configurations and to find a correlation between design parameters and optimal flow. The results of this analysis were applied in designing a screen shape for the Tulameen River project.

### 3.1 Background

Inclined screens have been used before to separate liquids from solids with the solids transported downstream and liquids sheared off the lower surface. The mining and wastewater industries have used wire screens for such a purpose. Coanda screens differ by their screen wire orientation. Rather than running parallel to the flow of water, the screen panels use tilted wires (Wahl, 2003). Figure 21 shown previously illustrates the primary features of the Coanda screen.

In describing the process, according to Wahl, water “flow passes over the crest of the weir, across a solid acceleration plate, and then across the screen panel, which is constructed of wedge-wire with the wires oriented horizontally, perpendicular to the flow across the screen.” Typically, an Ogee shape profile is used to provide a smooth acceleration of flow as it drops over the crest, delivering a flow tangent to the screen surface.

The flow passing over the screen is then collected in a conveyance channel and delivered to a penstock in applications for hydro-electric power generation. Flow velocities can be quite large, on the order of up to 2-3m/s. This velocity is dependent on the water drop height (or freeboard) described later. Figure 23 below shows a conceptual Coanda Screen application (Wahl, 2003).

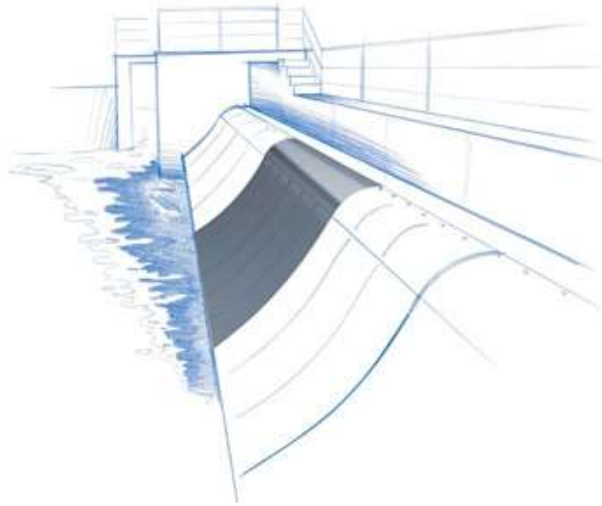


Figure 23 A typical Coanda-screen illustration (Bluslot Filter, 2020)

### 3.2 Debris Control

The Coanda screen is a self-cleaning type of intake that uses a unique type of “wedge-wire” panel in which the wires are tilted a few degrees in the downstream direction, following an Ogee-shaped slope (Figure 24).

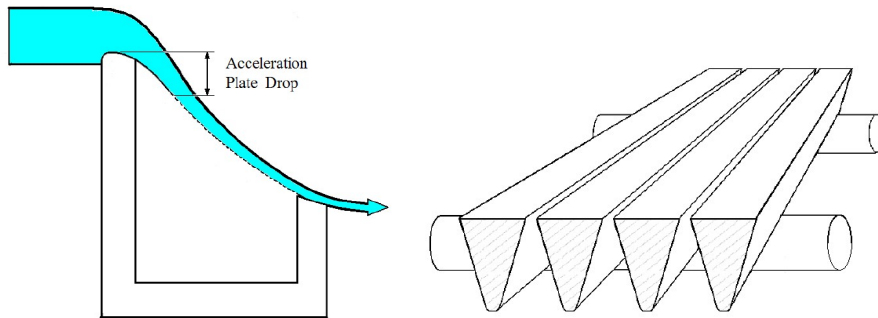
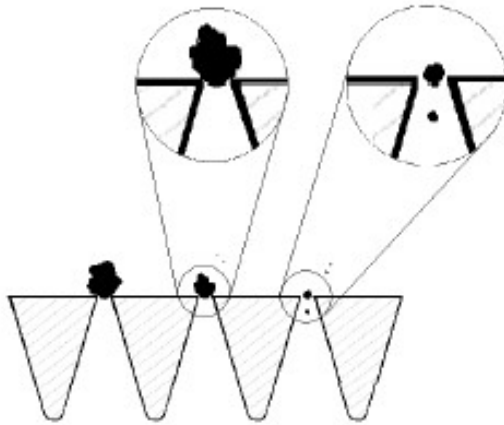


Figure 24 Wedge-wire profile

A solid acceleration plate forms the lead-in slope to the screen, creating the necessary water velocities for self cleaning.

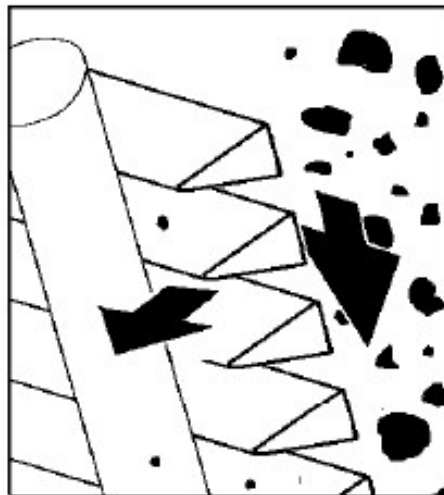
The close spacing of the wires (slot openings) allows the water to pass while retaining the debris on the screen with most screens filtering debris down to 1.0mm in diameter.

Figure 25 shows how a wedge-wire screen will prevent particles larger than the slot opening from entering. The open tapered slot of the wedge prevents particles that have entered through from getting stuck.



*Figure 25 Slot openings of the wedge-wire screen*

In order to keep the top area free from debris, the screens are oriented on a slope (Figure 26). Some of the water flows through the slot openings (orifice flow) and some of the water sweeps debris down the screen. The Coanda Screens need a minimum water velocity to clean the debris off.



*Figure 26 Oriented slope of the screens*

The solution to balance the velocity needed to sweep off the debris while also maintaining optimal orifice flow (through the screen) is to use tilted wedge wire screens. Rather than having the top surface of each wire flattened and parallel, each wire is slightly tilted. The leading edge of each wedge-wire sticks up into the flow (Figure 27) and cuts a section of water above it. This is called the shearing flow and as the water velocity across the screen increases, the shearing flow increases. Note that shearing flow is a type of orifice flow but differs due to the tilted wires.

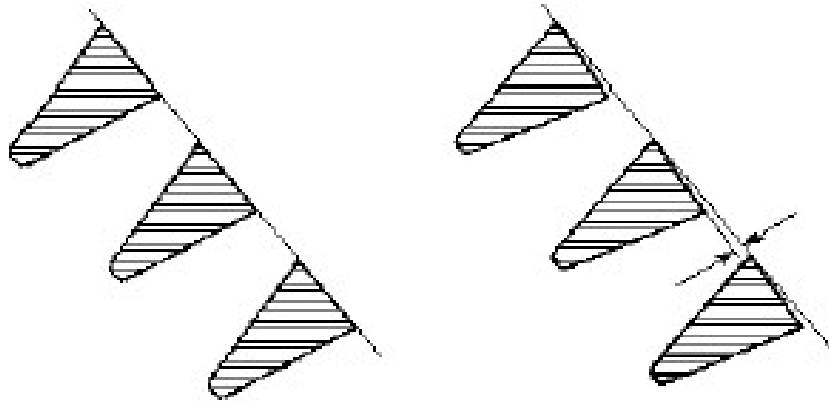


*Figure 27 Wedge-wire tilt from horizontal*

Figure 28 shows the flow difference where water is flowing across the face of two types of screens. This difference is much greater as the water speed increases across the screen face as the shear flow increases.

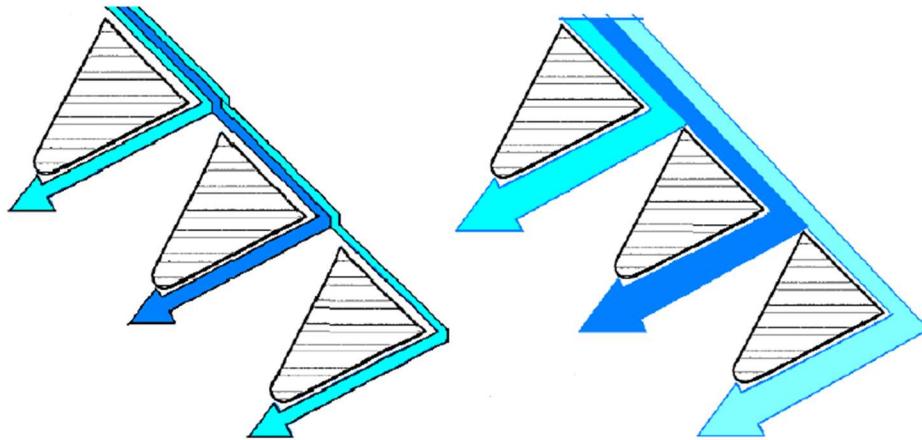


*Figure 28 The effect of tilting wires on orifice flow*

Water flows through the tilt wire screen into a collection chamber underneath (Figure 29). The chamber then flows into a pipe (penstock). The wedge-wire screen keeps debris above the screen and then swept downstream. Larger quantities of debris occur during spring run-off or after heavy rains. At these times there is also excess water to sweep the debris off the screens and carry them downstream.

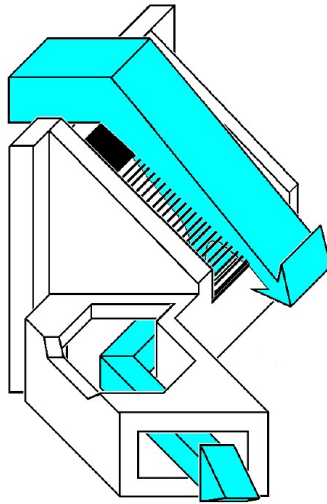


Figure 29 Collection chamber

The design of the accelerator plate is crucial in ensuring ideal water velocity is reached. The acceleration plate drop ( $H_a$ ) (Figure 30) creates the minimum water speeds needed for self cleaning (Douglass).

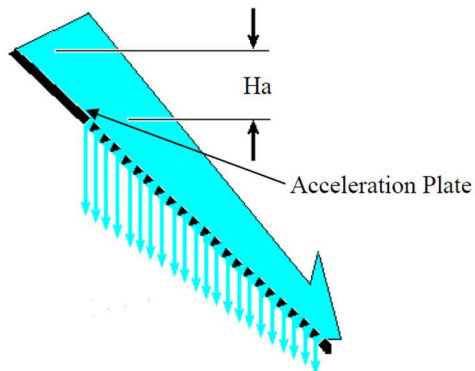


Figure 30 Accelerator plate drop height

The acceleration plate is a solid smooth plate above the screen. The acceleration plate also smooths the water and delivers accelerated water to the screen at the correct angle (Douglass).

### 3.3 Design Parameters

The following design parameters have been determined to affect the Coanda-Screen capacity. Most are related to the structure.

- Drop height from upstream flow above top of screen (top of weir)
- Screen Slope
- Curvature (arc radius) of screen
- Length of screen

Other properties known to affect design are the screen's

- Slot width
- Wire width
- Wire tilt angle (Wahl, 2003)

The design only focused on the first four primary parameters, assuming no backwater pressure and that the tailwater depth is below the toe of the structure.

### 3.4 Screen Capacity Theory

The Coanda-effect screen capacity is expressed as the discharge passing through the screen surface per unit width of crest. There are three types of discharge:

- Inflow to the screen (flow over the crest)
- Flow through the screen (unit discharge)
- Bypass flow over the screen (discharged down to the toe)

At very low flow rates on the river, almost all the inflow will pass through the screen and there is no bypass flow. A portion of the downstream is therefore dry. However, during most of the operation, flow through the screen and bypass flow will occur (Wahl, 2003).

### 3.5 Implementation & Calculations

The Coanda Screen design is based on research provided by the US Department of the Interior. Experimental results were consulted in order to optimize the best screen configuration. For the design of the weir proposal, an average flow of 30 m<sup>3</sup>/s was taken as the annual average discharge for the Tulameen River. This average value is conservative given that higher peak flooding rates have been known to occur.

The weir structure is modelled similarly to an Ogee Spillway (Figure 31) in shape and size. For a given discharge,  $Q$ , the freeboard or head can be calculated using Equation 3 (shown earlier):

$$Q = C * L * H^{3/2} \quad (3)$$

where L is the length of the weir, H is the head over the weir crest, and C, the discharge coefficient is given by

$$C = 2/3^{3/2} * g^{1/2}$$

where  $g = 9.81 \text{ m/s}^2$  is the acceleration due to gravity.

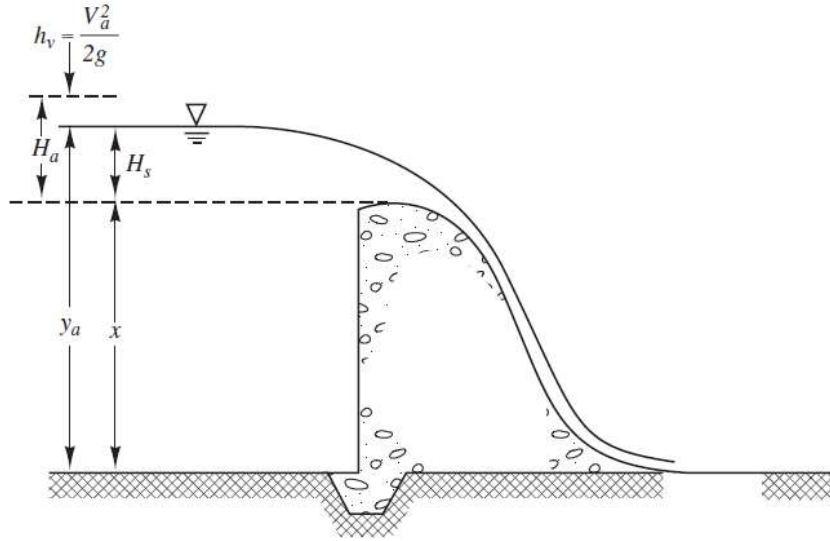


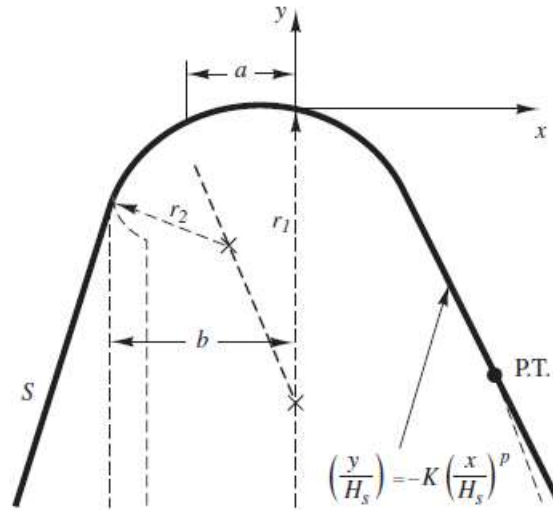
Figure 31 Flow profile over a weir spillway (Houghtalen, Akan, & Hwang, 2010)

Using Equation 3 for this design, a head of 0.40 meters was calculated with the backwall height, x, designed at 2.0 meters to reduce the impact on the river's backwater depth, (refer to Section 2.3).

### 3.6 Designing the Ogee Curve

The ideal accelerator plate profile will match an Ogee shape – the trajectory of a free-falling jet of water passing over a weir under its own gravity. This shape fully supports the trajectory as it passes over the weir. The shape differs for each discharge and upstream flow depth (Houghtalen, Akan, & Hwang, 2010).

The Ogee shape is best described by a power equation so that slope increases with the velocity of the free-falling water. In order to match the accelerator plate to the correct drop height, the Ogee profile was calculated so the plate's angle of incline matches the Ogee profile.



Upstream slope (vertical /horizontal)

|           | 3/0   | 3/1   | 3/2   | 3/3   |
|-----------|-------|-------|-------|-------|
| $a/H_s$   | 0.175 | 0.139 | 0.115 | 0     |
| $b/H_s$   | 0.282 | 0.237 | 0.214 | 0.199 |
| $r_1/H_s$ | 0.50  | 0.68  | 0.48  | 0.45  |
| $r_2/H_s$ | 0.20  | 0.21  | 0.22  | –     |
| $K$       | 0.500 | 0.516 | 0.515 | 0.534 |
| $p$       | 1.850 | 1.836 | 1.810 | 1.776 |

Figure 32 Ogee Profile (Houghtalen, Akan, & Hwang, 2010)

It should be noted that the design of the flow was set at 30 m<sup>3</sup>/s, yet it is recommended that the Ogee shape should be designed for a maximum expected annual flow (Wahl, 2003). At lower discharges the flow will be supported by the crest and will be delivered tangent to the screen surface, while the flow separation (shear) doesn't happen until much larger heads are reached.

Despite this recommendation, the design adhered to a discharge of 30 cumecs. The rationale was that design for any larger discharges will require a larger concrete weir construction, which would off-set the proposed cost savings of a Coanda screen.

From applying (the Ogee Spillway) Equation 3 above,  $H_s = 0.40\text{m}$  and from Figure 32 above, for an incoming slope of 3/1, Table 7 shows the resulting values of the incoming curve

Table 7 Ogee curve data

|                          |                          |
|--------------------------|--------------------------|
| $a = 0.139 H_s = 0.0556$ | $r_1 = 0.68 H_s = 0.272$ |
| $b = 0.237 H_s = 0.0948$ | $r_2 = 0.21 H_s = 0.084$ |
| $K = 0.516$              | $P = 1.836$              |

and the downstream curve equation is given by:

$$\left(\frac{y}{H_s}\right) = -K \left(\frac{x}{H_s}\right)^P = -0.516 \left(\frac{x}{H_s}\right)^{1.836} \quad (11)$$

The downstream end of the profile curve was then matched to three different straight slopes of 35, 45 and 60 degrees. The optimal slope was selected based on optimal screen

capacity. Taking derivatives of the above equation and setting this at the point of tangency to -1 (for a 45° slope as an example) yields,

$$d\left(\frac{Y}{H_s}\right) / d\left(\frac{X}{H_s}\right) = -KP\left(\frac{X}{H_s}\right)^{P-1} = -0.9474\left(\frac{X}{H_s}\right)^{0.836} = -1$$

Solving for X and Y, results in:

$$\left(\frac{X}{H_s}\right) = 1.067; X_{pt} = 0.4267m$$

$$\left(\frac{Y}{H_s}\right) = -0.516\left(\frac{x}{H_s}\right)^{1.836} = -0.516(1.067)^{1.836} = -0.5812; Y_{pt} = -0.2324m$$

The downstream section was then constructed based on Figure 33 below with the x and y coordinates calculated according to the above equations and Table 8.

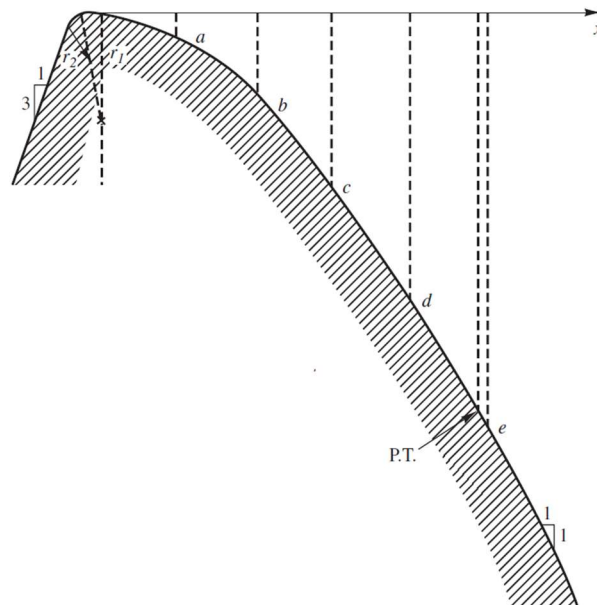


Figure 33 Ogee compound curve trajectory (Houghtalen, Akan, & Hwang, 2010)

Table 8 Ogee curve coordinates

| Point | x/Hs     | x        | y/Hs     | y        |
|-------|----------|----------|----------|----------|
| a     | 0.411583 | 0.164633 | -0.10111 | -0.04044 |
| b     | 0.823166 | 0.329267 | -0.36098 | -0.14439 |
| c     | 1.23475  | 0.4939   | -0.75996 | -0.30398 |
| d     | 1.646333 | 0.658533 | -1.28877 | -0.51551 |
| e     | 2.057916 | 0.823166 | -1.94135 | -0.77654 |

From several design iterations, the 45° incline was chosen with a planar screen length of 1.25m. The planar screen is superior to a concave screen for low head (<1m) applications.

The Ogee spillway profile (also in Appendix K: Ogee Profile) is shown below and from Figure 34, an accelerator plate drop of 23cm and tilt at an incline of 45° is appropriate. This design was based on an inflow of 30 m<sup>3</sup>/s over a 70m width, and a design discharge of 0.43 m<sup>3</sup>/s/m.

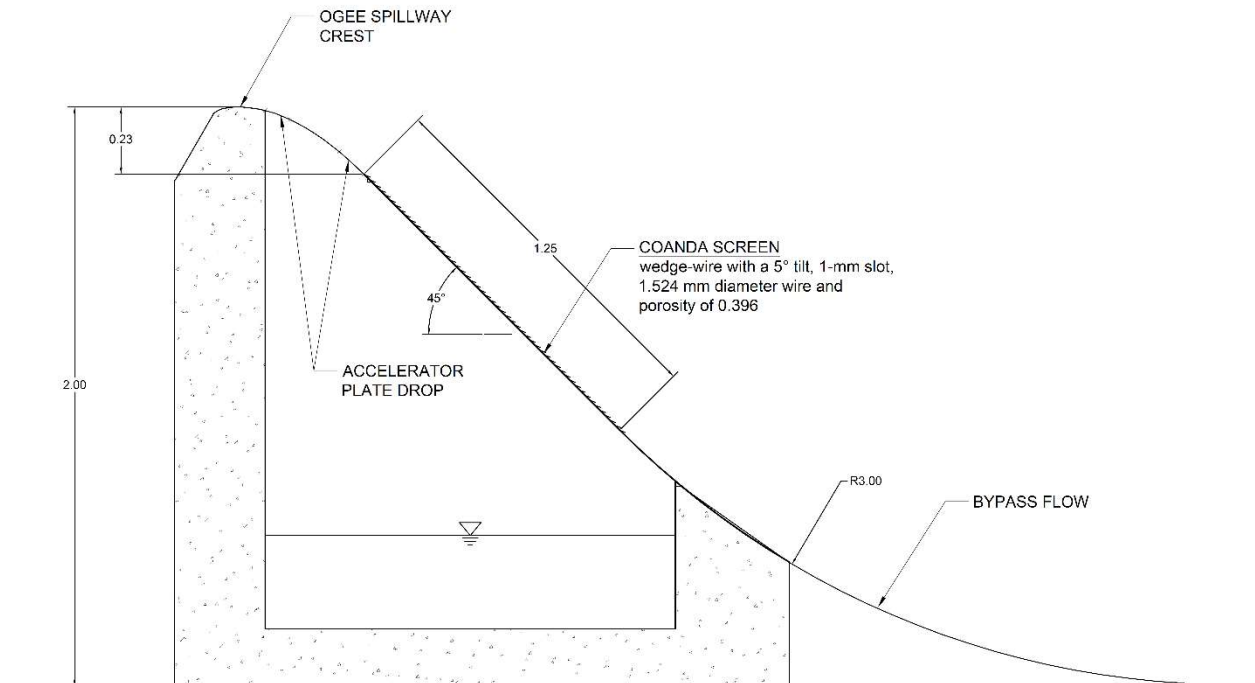


Figure 34 Optimal Coanda profile

This optimal size was based on empirical results conducted by the US Department of the Interior and is recommended for the proposal.

Figure 35 below shows that for a corresponding accelerator plate drop associated with a 45° incline angle and a 0.43 m<sup>3</sup>/s/m unit discharge, that a value of approximately 22-23cm is expected. This value corresponded to the Ogee spillway crest drop as calculated previously.

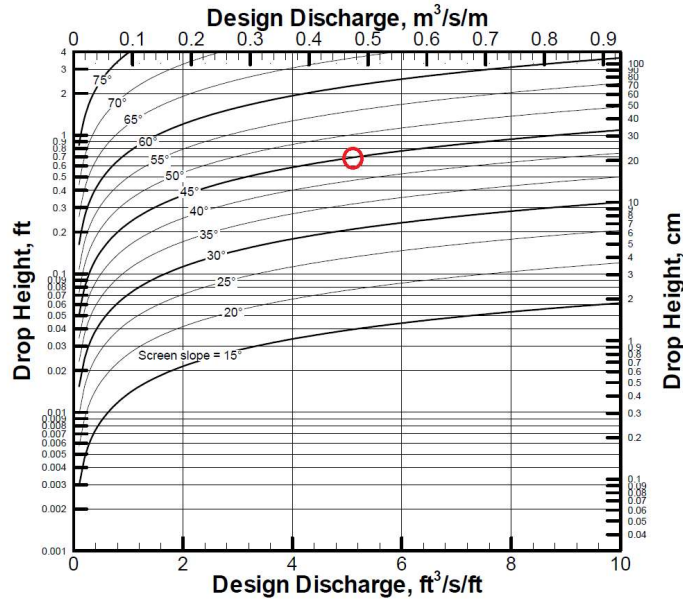


Figure 35 Discharge vs. Drop Height (Wahl, 2003)

Now based on experimental results, graphical interpolation was used to estimate the unit discharge, the orifice flow through the screen. Looking at Figure 36 below, for an accelerator plate drop of 23cm (0.23m), and by inferring linearly between 60 and 35 degrees (for a 45degree screen), a unit discharge of 0.225 m<sup>3</sup>/s/m can be expected.

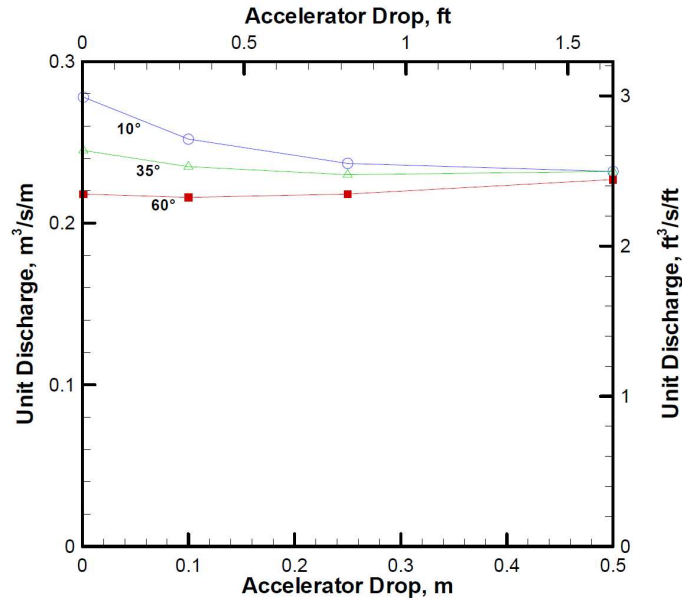


Figure 36 Unit Discharge vs. Accel. Drop (Wahl, 2003)

The reason for these differences is that the flatter screens have a larger component of orifice flow and a smaller component of shearing flow. Orifice flow is further increased when the accelerator drop height is reduced, since this increases the depth of flow above the screens. “For a steeper screen, shearing flow is more dominant, and shearing flow is increased as the drop height increases since this increases the velocity across the screen” (Wahl, 2003).

Once satisfied with a unit discharge of  $0.225 \text{ m}^3/\text{s}/\text{m}$  and an incline angle of  $45^\circ$ , Figure 37 was used to estimate the length of screen required. For a  $45^\circ$  angle and given discharge, a screen length of approximately 1.1 meters was interpolated.

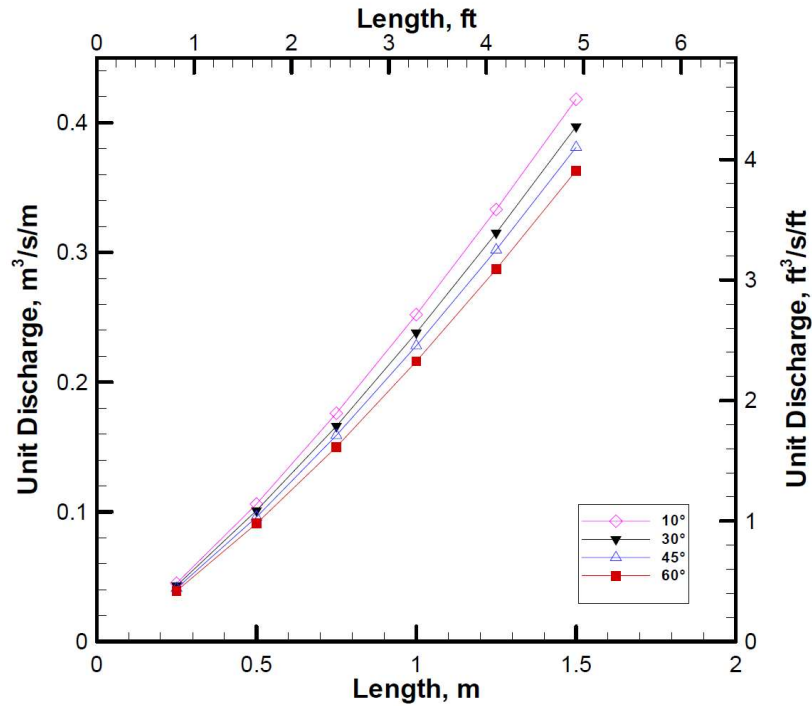


Figure 37 Unit Discharge vs. Screen length (Wahl, 2003)

However, screening capacity has been shown to increase non-linearly with increasing length and to specifically be proportional to  $L^{1.24}$ , with L being the length of the screen. So, a slightly longer screen of 1.25m was selected based on the above experimental results.

To select the optimal screen size, Figure 38 below was also analyzed. For the same input parameters of unit discharge and screen tilt, the best screen would have a wedge-wire with a 5° tilt, 1-mm slot, 1.524 mm diameter wire and porosity of 0.396.

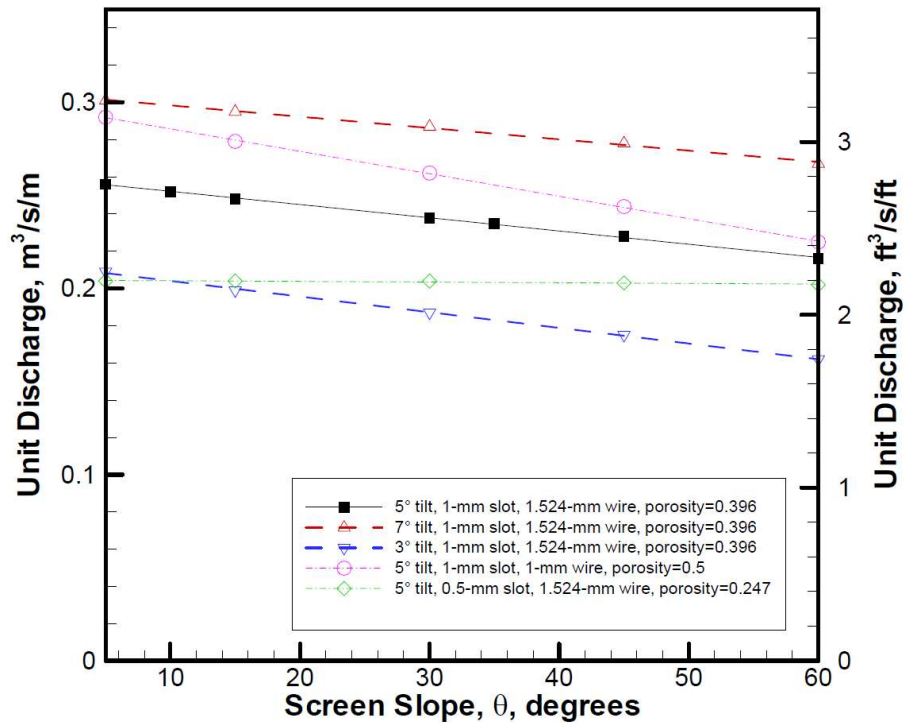


Figure 38 Unit Discharge vs. Screen slope (Wahl, 2003)

This analysis concluded the design of the Coanda Screen for a 30 m<sup>3</sup>/s average discharge with a freeboard of 0.4 meters.

### 3.7 Concrete Structure

The 70m wide concrete structure utilizes two angled wing walls and two parapet structures on both sides. These structures are for maintenance access with the east side for conveyance of unit discharge to the proposed hydro-station. The wing wall height was designed to accommodate a maximum instantaneous flow of 200m<sup>3</sup>/s as the water level is expected to rise about 2.5-3m for this amount of discharge.

A 2.0m high concrete backwall for the weir will be used with a 9m x 70m x 0.8m deep slab underlain for stability. It is recommended that a 2.5 m deep steel sheet pile be embedded at the heel of the slab to decrease groundwater conductivity and uplifting forces. Figure 39 below shows an isometric view and a front view of the proposal.

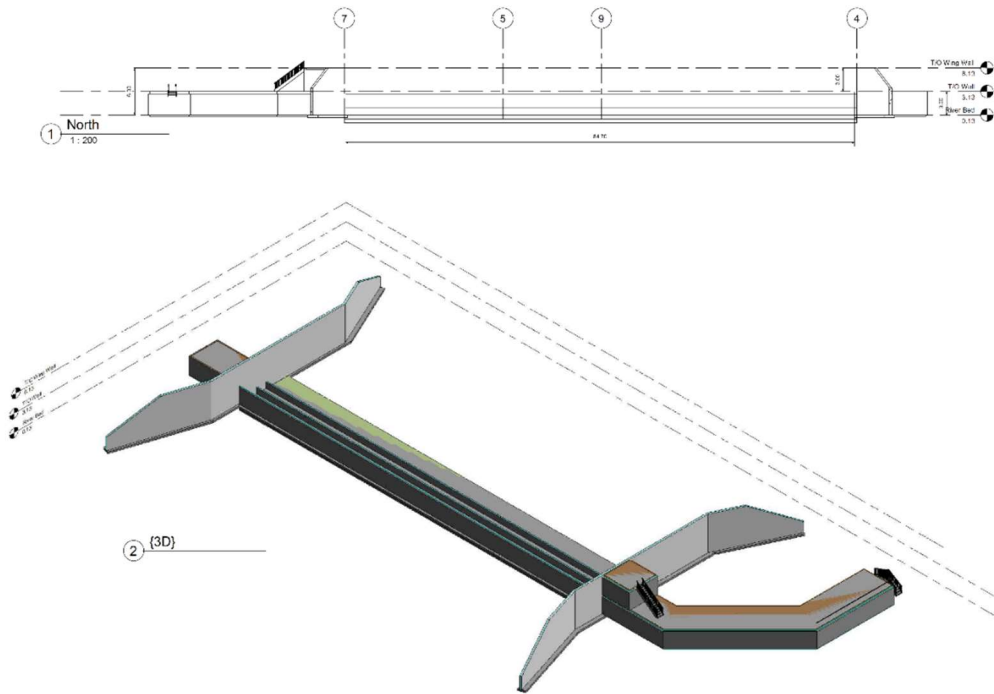


Figure 39 Proposed concrete structure

It is also recommended that at the toe of the footing a geotextile filter be used to prevent soil erosion than can lead to an increase in the hydraulic gradient.

An aerial rendering of the proposal is shown below in Figure 40 and Figure 41.



Figure 40 Overhead view of the weir structure



Figure 41 Another view of the structure

### 3.8 Unit Discharge and Hydropower

The output of energy at a dam is determined by the volume of water (discharge) released and the vertical distance it falls (head). A given amount of water falling a fixed distance will therefore produce a certain amount of energy. The head and the discharge based at the proposed hydro-station and the rotational speed of the generator can be used to select an appropriate turbine (United States Department of the Interior, 2005)

This report only focused on determining the potential power output from the hydro-station. This was based on an optimal unit discharge of  $0.225 \text{ m}^3/\text{s}/\text{m}$  as calculated in section 3.6.

The input head produces a water pressure and the greater the head, the greater the pressure to drive the turbines. Figure 42 below shows a schematic of a run-of-the-river assembly with a downstream powerhouse.

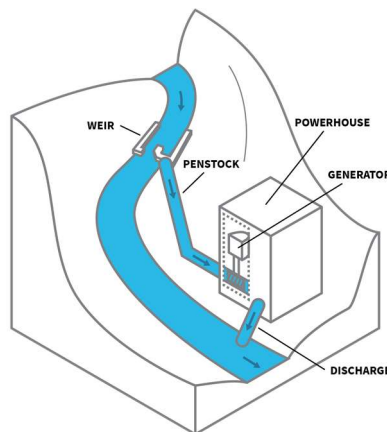


Figure 42 Powerhouse schematic (FirstLight Power, 2021)

To find the theoretical power (the measure of mechanical energy), the below equation can be used:

$$Power = \gamma Q h_t \quad (12)$$

where

$\gamma$  is the specific weight of water in  $kN/m^3$

$Q$  is the unit discharge in  $m^3/s$

and  $h_t$  is the head in  $m$ .

Due to economic considerations and environmental conditions, this design was for a low-head dam. In contrast to large-scale dams, new low-head dams have the ability to generate power close to where it is needed, and therefore reduce the power that is lost during transmission (Afework, et al.).

Assuming no head-loss in the conveyance pipe and near 100% efficiency in the turbine and generator, an approximate power output was estimated. The delivered head was estimated as 0.90 meters.

This drop of 0.90 meters was based on a tentative location of the hydro-station about 275m away from the weir as shown in Figure 43 below and by using Equation 2:

$$h_t = slope \times distance = 0.0033 \times 275m = 0.908 \cong 0.90 m$$



Figure 43 Tentative location for powerhouse

The power output was then computed using equation 11.

$$Power = \frac{9.81kN}{m^3} * 0.225 \frac{m^3}{s} * 70m * 0.9m = 139 kW$$

This output, even when considering near perfect efficiency, qualifies this station as on the lower end of a mini run-of-the-river station (Table 9). However, this is based on an average design flow of 30 cumecs, and throughout the year, there will be positive and negative fluctuations in this value.

*Table 9 Classification of run-of-the-river stations*

| <b>Classification</b> | <b>Capacity</b> |
|-----------------------|-----------------|
| Micro                 | < 100 kW        |
| Mini                  | 100 kW – 1MW    |
| Small                 | 1 – 50 MW       |

To increase the power output, a larger drop in head can be designed with the station located further downstream to achieve a greater elevation change.

## 4.0 CONCLUSION

A weir structure was designed for use on the Tulameen River near Princeton. The purpose was to find a suitable site location and to analyze the feasibility of using it for hydro-electric power generation.

To begin, an analysis of the river flow captured the particulars of what amount of discharge could be expected by using various data from a water gauge station. This data was analysed using the Gumbel Method to determine the peak run-off for a 100-year return flood which would raise the water level by about 3 meters.

Based on an average annual flow of 30 m<sup>3</sup>/s, the weir site location was analyzed using Manning’s Equation to determine energy changes and how the concrete design would need to address these. Wingwalls were designed to accommodate a river depth change up to 5m in height and the span of 70m was calculated based on an optimal design freeboard of 0.4m from the Ogee Spillway Equation.

A 2m high backwall would affect the backwater river profile up to about 474 meters upriver with a depth transition from 2.4m to 0.91m. The Kettle Valley Rail bridge located upstream would not be affected by these changes.

A soil permeability analysis concluded that the concrete slab design (with sheet pile at the heel) was sufficient for preventing uplift with a factor of safety of 1.95.

Coanda-effect screens were selected as they are finding greater popularity for smaller low-head run-of-the-river applications and because of their reduced maintenance costs.

Based on studies and data provided by the United States Department of the Interior, an optimal Coanda screen configuration was determined to be a planar 1.25m screen tilted at 45degrees to horizontal with a 1.524 mm diameter wedge-wire screen having a 5° tilt, and 1-mm slot. An accelerator plate drop and Ogee profile were calculated and sketched as well.

The potential power output based on a near perfect efficiency and an incoming head of approximately 0.90m was calculated to be 139kW. This value is subject to change as river flows vary throughout the year and qualifies the station as a ‘mini’ generator.

Based on the results of the above, the proposal appears to meet the requirements set out by the Town of Princeton. Further recommendations and criteria to be explored are addressed in the section on recommendations.

## 5.0 RECOMMENDATIONS & DISCUSSION

Run-of-the-river hydro contributes very little to hydro-carbon emissions. Most of the emissions are actually due to the construction of the system itself as it relies mostly on the natural conversion of gravitational and kinetic energy into electro-mechanical energy. So, there are very few operational emissions (Afework, et al.).

Compared to larger dams, the smaller amount of water storage results in a “smaller environmental footprint,” and although there are fewer emissions compared to those that rely on fossil fuels, there are other environmental impacts.

The “manipulation of river flows” (Afework, et al.) can alter how the aquatic ecosystem works, especially in regards to fish migration patterns. But due to the relatively low head of the design and the implementation of the Coanda screen, fish are able to successfully migrate downstream past the system without having their route interrupted (Appendix A: Fish Bypass). For upstream migration, it is recommended that consideration be given to a fish ladder component.

Another aspect to consider is the thermal pollution of the water downstream of the hydro-station. As water is injected back into the river, it will have a higher “turbidity” that may cause thermal pollution and interrupt part of the ecosystem.

Thought has been given to the design of the weir structure and incorporating a stilling basin of cobbles will further reduce the hydraulic head downstream. This has the effect of reducing soil erosion, another environmental affect that must be considered. Figure 44 below shows a typical stilling basin.



*Figure 44 Weir with stilling basin (Knight Piesold Consulting, 2021)*

The back water profile curve was calculated to extend 474m upstream of the structure, coming far short of the Kettle Valley Rail Bridge. However, raising the average depth of flow of the river could still have unforeseen environmental effects and additional research should be undertaken to investigate this.

Coanda screens are known to be low-maintenance but anecdotal evidence points toward wear-and-tear of the screens and eventual sediment accumulation on the screens. To counter this, a sluice gate is also recommended to provide bypass for water control and the release of sediment buildup.

Another point of concern is the effect of flooding from a 200-year event. According to the discharge calculations, a flood of this order of magnitude would submerge the weir structure and the structural ramifications of such an event have not been assessed in this report. It is recommended that such an undertaking be deferred to specialists in that field.

According to (Afework, et al.), “it is difficult to determine in general whether or not the damage inflicted on the environment by run-of-the-river systems is outweighed by the relatively small output as compared to large hydro dams. That means that each project must be evaluated on the specific details of the hydroelectric power plants being proposed”.

## 5.1 Comparison to Traditional Hydro

A run-of-the-river design was favoured for this proposal compared to a traditional hydro dam. Traditional hydro dams are generally more expensive and take a lot longer to construct (Afework, et al.). Run-of-the-river structures also do not suffer as much from issues of flooding, since the pondage, or backwater pooling is much less than that for a dam.

## 5.2 River Flood Analysis

The river flood analysis was based on a 100-year storm but in some cases, a 200-year return might be recommended. The peak discharge rate of  $650\text{m}^3/\text{s}$  is a large value and can potentially raise the river depth by 4-5 meters. It is recommended that further investigations be conducted by hydrological specialists to see how this might affect other parts of river and what affect it might have on the hydro station itself.

## REFERENCES

- Afework, B., Cey, E., Goodfellow, L., Hanania, J., Stenhouse, K., & Donev, J. (n.d.). [https://energyeducation.ca/encyclopedia/Run-of-the-river\\_hydroelectricity](https://energyeducation.ca/encyclopedia/Run-of-the-river_hydroelectricity). Retrieved February 2021
- Bluslot Filter. (2020, January). <https://meshfiltro.com/coanda-screen/>. Retrieved February 2021
- Coduto, D. P., Yeung, M.-c., & Kitch, W. A. (2011). *Geotechnical Engineering Principles and Practices* (2nd ed.). Upper Saddle River, NJ: Prentice Hall.
- Douglass, S. (n.d.). Retrieved February 2021, from [www.coandaintakes.com](http://www.coandaintakes.com).
- FirstLight Power. (2021). <https://www.firstlightpower.com/about-hydro/>. (F. Power, Producer) Retrieved March 2021
- Google Earth. (2021). Kettle Valley Rail Bridge. Retrieved February 21st, 2021
- Government of Canada. (2021). *Real-Time Hydrometric Data for Tulameen River at Princeton*. Retrieved February 2021, from [https://wateroffice.ec.gc.ca/search/real\\_time\\_e.html](https://wateroffice.ec.gc.ca/search/real_time_e.html).
- Hay & Company Consultants Inc. (1995). *Floodplain Mapping Program*. Design Brief, Vancouver.
- Houghtalen, R. J., Akan, A. O., & Hwang, N. H. (2010). *Fundamentals of Hydraulic Engineering Systems* (4th ed.). Prentice Hall.
- Knight Piesold Consulting. (2021). <https://www.knightpiesold.com/en/expertise/power/hydropower/>. Retrieved February 2021
- Lord, T. M., & Green, A. J. (1974). *Soils of the Tulameen Area of British Columbia*. Canada Department of Agriculture.
- Mefford, B. (2013). *Guide to Fish Screens*. U.S. Bureau of Reclamation, United States Department of Agriculture, Denver.
- Regional District of Okanagan - Similkameen. (2021). <https://maps.rdos.bc.ca/Html5Viewer/?viewer=publicparcels>. Retrieved February 2021, from <https://maps.rdos.bc.ca/portal/apps/sites/#!/data>.
- United States Department of Agriculture. (2007). *Stream Hydrology*. Engineering Handbook.
- United States Department of the Interior. (1987). *Design of Small Dams* (3rd ed.). U.S. Government Printing Office.
- United States Department of the Interior. (2005, July). *Hydroelectric Power*.
- Wahl, T. L. (2003). *Design Guidance for Coanda-Effect Screens*. United States Department of the Interior, Water Resources Services, Denver.

## APPENDICES

### Appendix A: Fish Bypass

Fish and debris are transported by non-diverted flow passing over the Coanda screen surface, precluding the need for fish ladders.

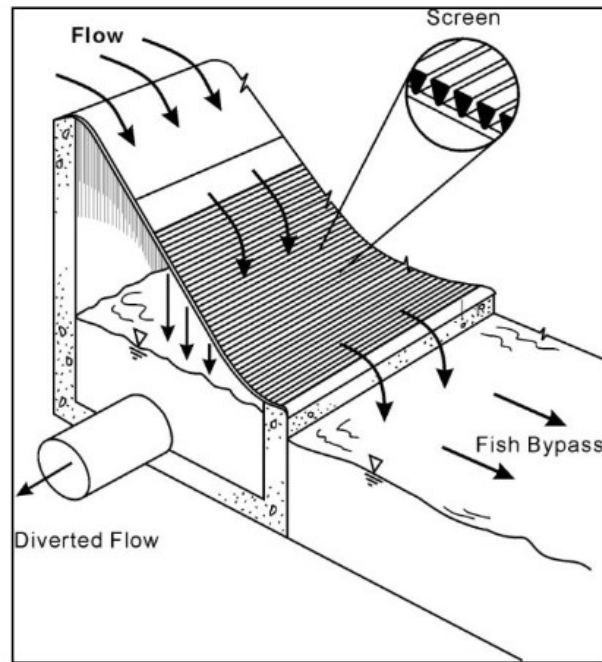


Figure 45 Fish bypass (Mefford, 2013)

## Appendix B: Gauge Station

Table 10 Gauge Station (Government of Canada, 2021)

### Station Information

|                                  |   |                                 |                  |
|----------------------------------|---|---------------------------------|------------------|
| <b>Active or discontinued:</b>   | Active  | <b>Province / Territory:</b>    | British Columbia |
| <b>Latitude:</b>                 | 49° 27' 27" N   | <b>Longitude:</b>               | 120° 31' 06" W   |
| <b>Gross drainage area:</b>      | 1,780 km <sup>2</sup>   | <b>Effective drainage area:</b> | N/A              |
| <b>Record length:</b>            | 72 Years  | <b>Period of record:</b>        | 1950 - 2021      |
| <b>Regulation type:</b>          | Natural   | <b>Regulation length:</b>       | N/A              |
| <b>Real-time data available:</b> | Yes   | <b>Sediment data available:</b> | No               |
| <b>Type of water body:</b>       | River   | <b>RHBN:</b>                    | No               |
| <b>EC Regional Office:</b>       | VANCOUVER   | <b>Current Operation</b>        | Continuous       |
|                                  |   | <b>Schedule:</b>                |                  |
| <b>Data contributed by:</b>      | N/A   | <b>Operation Period:</b>        | JAN - DEC        |
| <b>Datum of published data:</b>  | ASSUMED DATUM   |                                 |                  |
| <b>To convert to:</b>            | CANADIAN GEODETIC<br>VERTICAL DATUM<br>2013:EPOCH2010, add<br>636.046 m |                                 |                  |

## Appendix C: Tulameen Discharge & Depth

Data acquired from the gauge station was accessed from the Government of Canada's water-office website. Historical and real-time data can be accessed in graphical and numerical format. Graphical output is shown below in Figure 46 for the Tulameen River's depth and discharge rates for 2018.

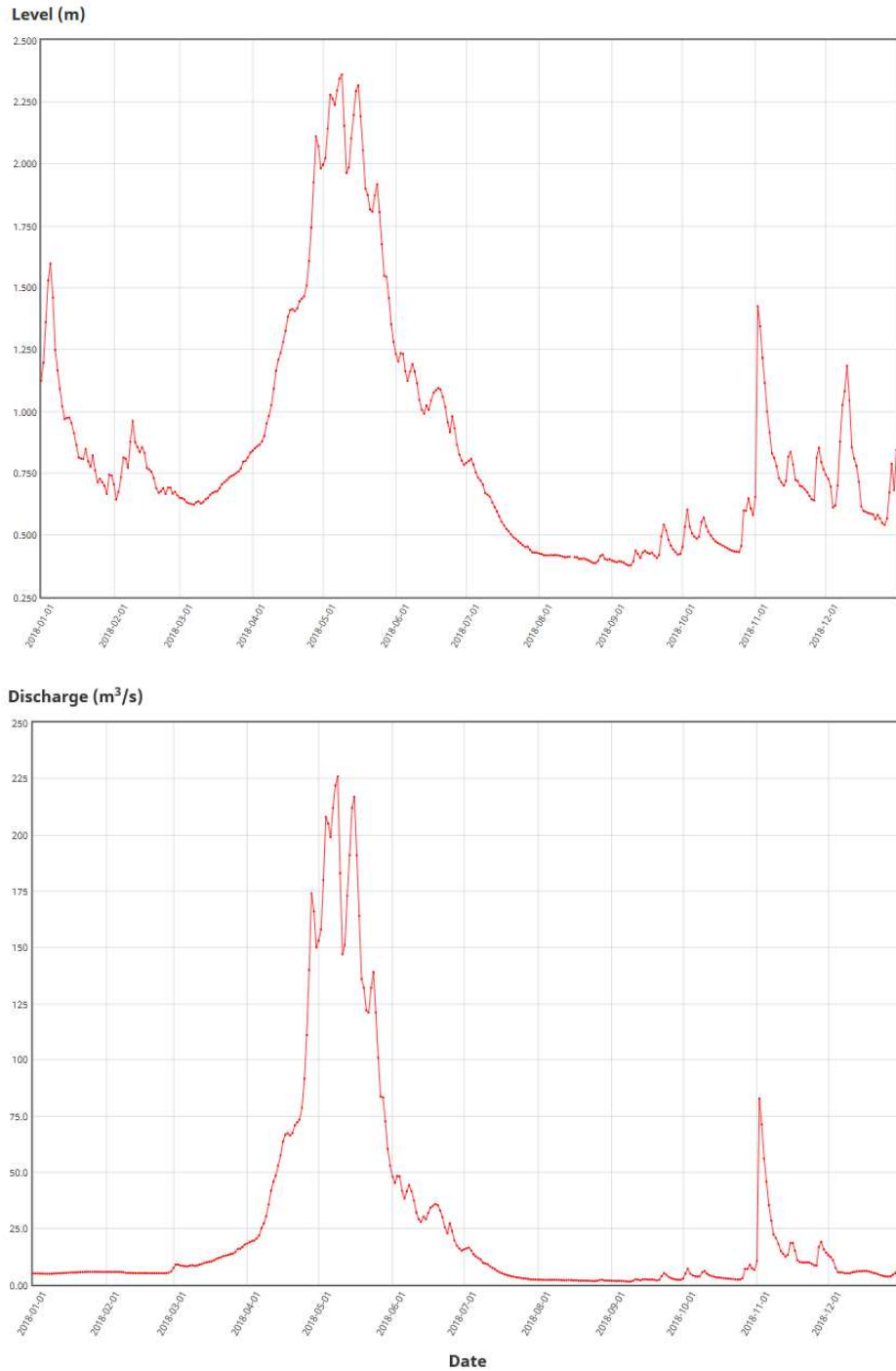


Figure 46 Depth & Discharge (Government of Canada, 2021)

## Appendix D: Manning Coefficients

Table 11 below shows the Manning Roughness Coefficients for various open channel surfaces.

*Table 11 Roughness coefficients (Houghtalen, Akan, & Hwang, 2010)*

| Channel Surface                                      | <i>n</i>    |
|--|-------------|
| Glass, polyvinyl chloride, high-density polyethylene | 0.010       |
| Smooth steel, metals                                 | 0.012       |
| Concrete   | 0.013       |
| Asphalt  | 0.015       |
| Corrugated metal                                     | 0.024       |
| Earth excavation, clean                              | 0.022–0.026 |
| Earth excavation, gravel or cobbles                  | 0.025–0.035 |
| Earth excavation, some weeds                         | 0.025–0.035 |
| Natural channels, clean and straight                 | 0.025–0.035 |
| Natural channels, stones or weeds                    | 0.030–0.040 |
| Riprap-lined channel                                 | 0.035–0.045 |
| Natural channels, clean and winding                  | 0.035–0.045 |
| Natural channels, winding with pools or shoals       | 0.045–0.055 |
| Natural channels, weeds with debris or deep pools    | 0.050–0.080 |
| Mountain streams, gravel or cobbles                  | 0.030–0.050 |
| Mountain streams, cobbles or boulders                | 0.050–0.070 |

## Appendix E: Trapezoidal Channel Calculations

Table 12 Calculations of existing channel section

| Data from 2018 discharge and depth |  |       |                   |  |
|------------------------------------|--|-------|-------------------|--|
|                                    | Q1=  | 4.32  | m <sup>3</sup> /s |  |
|                                    | Q2=  | 3.52  | m <sup>3</sup> /s |  |
|                                    | d1=  | 0.45  | m                 |  |
|                                    | d2=  | 0.41  | m                 |  |
|                                    | b=   | 5.00  | m                 |  |
| (guess)                            | m/1=   | 33.58 |                   |  |
|                                    | Area1=   | 8.98  | m <sup>2</sup>    |  |
|                                    | Area2=   | 7.70  | m <sup>2</sup>    |  |
|                                    | Pw1=   | 35.10 | m                 |  |
|                                    | Pw2=   | 32.55 | m                 |  |
|                                    | Rh1=   | 0.26  | m                 |  |
|                                    | Rh2=   | 0.24  | m                 |  |
|                                    |  |       |                   |  |
|                                    | Q1/Q2=   | 1.23  |                   |  |
|                                    |  |       |                   |  |
|                                    | <b>Use Solver to find m</b>                    |       |                   |  |
|                                    | Area1/Area2=                                   | 1.17  | m <sup>2</sup>    |  |
|                                    | Rh1/Rh2 =                                      | 1.08  |                   |  |
|                                    | target=  | 1.23  |                   |  |
|                                    |  |       |                   |  |
|                                    | Use Goalseek for rectangular channel to find b |       |                   |  |
|                                    |  |       |                   |  |
| Top Width                          | T=   | 35.1  | m                 |  |

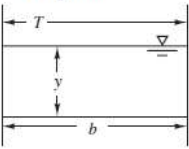
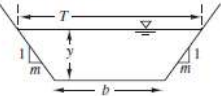
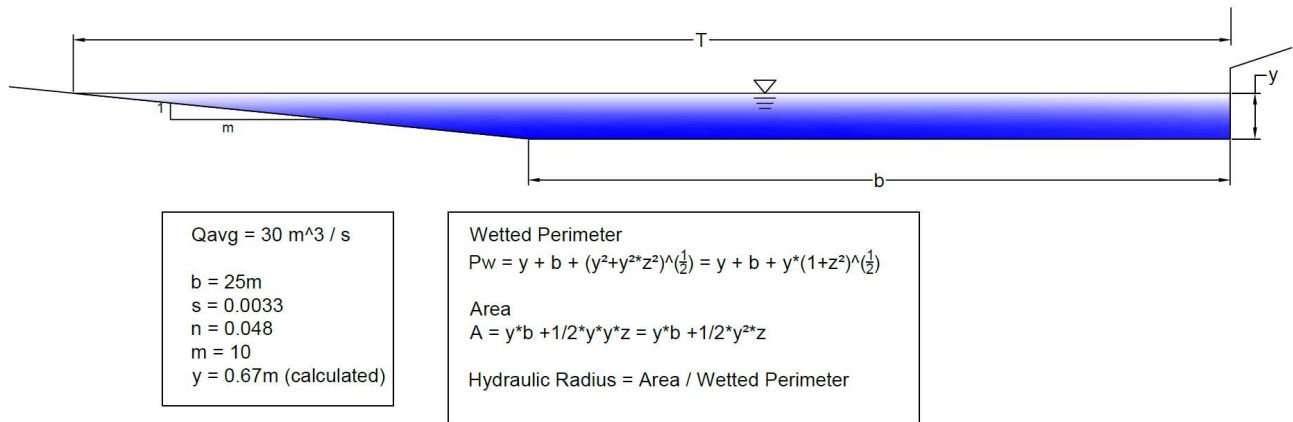
| Section Type   | Area (A)    | Wetted perimeter (P)   | Hydraulic Radius ( $R_h$ )               | Top Width (T) | Hydraulic Depth (D)         |
|--|-------------|------------------------|--|---------------|-----------------------------|
| Rectangular<br> | $by$        | $b + 2y$               | $\frac{by}{b + 2y}$                      | $b$           | $y$                         |
| Trapezoidal<br> | $(b + my)y$ | $b + 2y\sqrt{1 + m^2}$ | $\frac{(b + my)y}{b + 2y\sqrt{1 + m^2}}$ | $b + 2my$     | $\frac{(b + my)y}{b + 2my}$ |

Figure 47 Open channels (Houghtalen, Akan, & Hwang, 2010)

## Appendix F: Trapezoidal Section at Site



Using an iterative solver, the normal depth of flow was calculated as 0.667m as shown below in Table 13.

Table 13 Normal flow depth

| Unaltered Section View |        |                              |
|------------------------|--------|------------------------------|
| <b>n =</b>             | 0.048  | <i>previously calculated</i> |
| <b>s =</b>             | 0.003  |                              |
| <b>b =</b>             | 25.000 | m                            |
| <b>m =</b>             | 10.000 |                              |
| <b>Qavg =</b>          | 30.000 | m <sup>3</sup> /s            |
| <b>Find depth, y =</b> | 0.667  | m ( <i>Initial Guess</i> )   |
| <b>Area =</b>          | 18.898 | m <sup>2</sup>               |
| <b>Pw =</b>            | 12.370 | m                            |
| <b>Rh =</b>            | 1.528  | m                            |
| <b>Target Q</b>        | 30.000 | m <sup>3</sup> /s            |
| <b>T =</b>             | 31.669 | m                            |

## Appendix G: Yearly Peak Flow Data

The peak flow was reviewed over a 15-year period. A maximum design flow of 200m<sup>3</sup>/s was selected based on the below data taken from the water-office (Government of Canada, 2021).

Table 14 Peak annual discharge

| Peak Flow (cumecs)   |         |          |       |       |        |       |       |        |           |         |          |          |          |
|----------------------|---------|----------|-------|-------|--------|-------|-------|--------|-----------|---------|----------|----------|----------|
| Year                 | January | February | March | April | May    | June  | July  | August | September | October | November | December | Max flow |
| 2018                 | 5.74    | 5.89     | 17.9  | 174   | 226    | 48.4  | 16.5  | 2.26   | 5.15      | 7.15    | 82.8     | 12.3     | 226      |
| 2017                 | 2.94    | 4.86     | 14.9  | 54.8  | 185    | 131   | 15.3  | 2.31   | 1.14      | 30.7    | 95.9     | 4.95     | 185      |
| 2016                 | 20.7    | 23.5     | 29.6  | 176   | 104    | 36.9  | 8.72  | 4.31   | 2.78      | 16.4    | 14.3     | 2.56     | 176      |
| 2015                 | 46.2    | 53.7     | 49.9  | 44.9  | 57.5   | 28    | 4.31  | 4.51   | 8.21      | 21.1    | 53.5     | 28.8     | 57.5     |
| 2014                 | 8.97    | 6.38     | 18.3  | 48.1  | 190    | 127   | 39.4  | 5.6    | 4.04      | 10      | 19.2     | 33.5     | 190      |
| 2013                 | 3.6     | 3.5      | 20.4  | 54.3  | 247    | 93.7  | 34.4  | 5.4    | 20.6      | 13.5    | 11.6     | 6.97     | 247      |
| 2012                 | 5.78    | 6.67     | 4.89  | 151   | 155    | 149   | 93.5  | 7.98   | 2.41      | 36.8    | 44.8     | 7.04     | 155      |
| 2011                 | 7.68    | 5.79     | 4.81  | 6.97  | 128    | 172   | 74.6  | 14.9   | 13.4      | 10.1    | 6.21     | 3.55     | 172      |
| 2010                 | 9.25    | 4.8      | 11    | 68.3  | 127    | 110   | 31.2  | 4.51   | 11.5      | 6.02    | 14       | 14       | 127      |
| 2009                 | 2.58    | 2.5      | 2.72  | 41.8  | 127    | 97.8  | 12    | 4.98   | 2.97      | 23.2    | 50.5     | 25.8     | 127      |
| 2008                 | 5.5     | 4.4      | 4.33  | 15.6  | 232    | 119   | 44.3  | 13.9   | 5.29      | 13.3    | 41.4     | 13.7     | 232      |
| 2007                 | 9.6     | 9.62     | 124   | 84.1  | 134    | 150   | 27    | 4.54   | 1.9       | 19.2    | 12.7     | 35       | 150      |
| 2006                 | 12      | 5.23     | 5.56  | 74.1  | 206    | 79.8  | 11.4  | 1.87   | 1.05      | 7       | 242      | 12.7     | 242      |
| 2005                 | 121     | 29.6     | 34    | 71.7  | 43.9   | 17    | 10.2  | 2.11   | 14.6      | 26.8    | 12.7     | 14.6     | 121      |
| 2004                 | 6.05    | 5.3      | 20.9  | 97.2  | 113    | 63.2  | 9.99  | 3.34   | 16.2      | 7.69    | 52.9     | 61.4     | 113      |
| <b>Average</b>       | 17.84   | 11.45    | 24.21 | 77.52 | 151.69 | 94.85 | 28.85 | 5.50   | 7.42      | 16.60   | 50.30    | 18.46    |          |
| <b>Max on record</b> | 210     | 77.7     | 124   | 186   | 374    | 328   | 161   | 35.7   | 31.1      | 193     | 392      | 235      |          |

## Appendix H: The Standard Step Method

According to (Houghtalen, Akan, & Hwang, 2010), the standard step method is used to calculate gradually varied flow water surface profiles and employs a finite difference solution scheme to solve the differential, gradually varied flow equation.

It was used in this application with 10 step intervals and provided a backwater profile distance of about 474m. This value is shown in Table 15 below and assumes a trapezoidal cross section and a base width of 25m.

*Table 15 Output from the Standard Step Method*

| Trapezoidal Section | Depth - y (m) | Area A   | Wetted Perimeter Pw | Hydraulic Radius R | Velocity | Energy | Si      | S <sub>AVG</sub> | ΔL (m)  |
|---------------------|---------------|----------|---------------------|--------------------|----------|--------|---------|------------------|---------|
| 1                   | 2.4000        | 117.6000 | 53.2394             | 2.2089             | 0.2551   | 2.4033 | 0.00004 |                  |         |
| 2                   | 2.2349        | 105.8215 | 49.9213             | 2.1198             | 0.2835   | 2.2390 | 0.00005 | 0.00004          | 50.4262 |
| 3                   | 2.0698        | 94.5880  | 46.6032             | 2.0296             | 0.3172   | 2.0750 | 0.00006 | 0.00005          | 50.5541 |
| 4                   | 1.9048        | 83.8996  | 43.2850             | 1.9383             | 0.3576   | 1.9113 | 0.00008 | 0.00007          | 50.7361 |
| 5                   | 1.7397        | 73.7563  | 39.9669             | 1.8454             | 0.4067   | 1.7481 | 0.00012 | 0.00010          | 51.0023 |
| 6                   | 1.5746        | 64.1579  | 36.6488             | 1.7506             | 0.4676   | 1.5857 | 0.00017 | 0.00014          | 51.4055 |
| 7                   | 1.4095        | 55.1046  | 33.3307             | 1.6533             | 0.5444   | 1.4246 | 0.00024 | 0.00020          | 52.0446 |
| 8                   | 1.2444        | 46.5964  | 30.0126             | 1.5526             | 0.6438   | 1.2655 | 0.00037 | 0.00031          | 53.1225 |
| 9                   | 1.0793        | 38.6332  | 26.6945             | 1.4472             | 0.7765   | 1.1101 | 0.00059 | 0.00048          | 55.1164 |
| 10                  | 0.9143        | 31.2151  | 23.3763             | 1.3353             | 0.9611   | 0.9613 | 0.00101 | 0.00080          | 59.4292 |
|                     |               |          |                     |                    |          |        |         | sum =            | 473.84  |

## Appendix I: The Gumbel Method

The Gumbel Method is a type of frequency analysis often used in flood predictions. Peak flooding is observed from longitudinal data and then based on certain probability functions and frequency factors (Table 16), various extremes are extrapolated (United States Department of Agriculture, 2007). Such a method was implemented to estimate a peak discharge rate based on a 100-year return rain event with a K value (sample size) taken as forty for this project.

### Procedure

- i. List and arrange annual floods (x) in descending order of magnitude.
- ii. Assign rank 'm', m = 1 for highest value and so on.
- iii. Calculate return period (T) and/or probability of exceedance (P) by equations  $n + 1/m$  and  $m/n + 1$  respectively. These values together with respective flood magnitude give plotting positions.
- iv. Now calculate mean x and standard deviation S.
- v. From Table 16 of frequency factors for Gumbel method read off values for desired return periods (vi) and the available sample size.
- vi. Using relation  $x = x + KS$  calculate flood values for various return periods.
- vii. Using the extreme value probability paper plot the x values against respective return periods or P values and join the points to obtain the required frequency curve.

Table 16 Frequency Factors for Gumbel Method (United States Department of Agriculture, 2007)

| Sample size | Return period, T (yr) |       |       |      |      |      |      |      |      |
|-------------|-----------------------|-------|-------|------|------|------|------|------|------|
|             | 1.11                  | 1.25  | 2.00  | 2.33 | 5    | 10   | 25   | 50   | 100  |
| 15          | -1.34                 | -0.98 | -0.15 | 0.06 | 0.97 | 1.70 | 2.63 | 3.32 | 4.01 |
| 20          | -1.29                 | -0.95 | -0.15 | 0.05 | 0.91 | 1.63 | 2.52 | 3.18 | 3.84 |
| 25          | -1.26                 | -0.93 | -0.15 | 0.04 | 0.89 | 1.58 | 2.44 | 3.09 | 3.73 |
| 30          | -1.24                 | -0.91 | -0.16 | 0.04 | 0.87 | 1.54 | 2.39 | 3.03 | 3.65 |
| 40          | -1.21                 | -0.90 | -0.16 | 0.03 | 0.84 | 1.50 | 2.33 | 2.94 | 3.55 |
| 50          | -1.20                 | -0.88 | -0.16 | 0.03 | 0.82 | 1.47 | 2.28 | 2.89 | 3.49 |
| 60          | -1.18                 | -0.87 | -0.16 | 0.02 | 0.81 | 1.45 | 2.25 | 2.85 | 3.45 |
| 70          | -1.17                 | -0.87 | -0.16 | 0.02 | 0.80 | 1.43 | 2.23 | 2.82 | 3.41 |
| 80          | -1.16                 | -0.86 | -0.16 | 0.02 | 0.79 | 1.42 | 2.21 | 2.80 | 3.39 |
| 100         | -1.15                 | -0.85 | -0.16 | 0.02 | 0.77 | 1.40 | 2.19 | 2.77 | 3.35 |
| 200         | -1.11                 | -0.82 | -0.16 | 0.01 | 0.74 | 1.33 | 2.08 | 2.63 | 3.18 |
| 400         | -1.07                 | -0.80 | -0.16 | 0.00 | 0.70 | 1.27 | 1.99 | 2.52 | 3.05 |

Table 17 Frequency and Probability

| Year             | Annual Peak<br>Instaneous<br>Flow (m <sup>3</sup> /s) | Order<br>Number (m) | Return<br>Period, T<br>(years) | Probability |
|------------------|---|---------------------|--------------------------------|-------------|
|                  |   | m                   | (n+1)/m                        | (m)/(n+1)   |
| 1995             | 708   | 1                   | 41.00                          | 0.02        |
| 2006             | 502   | 2                   | 20.50                          | 0.05        |
| 1990             | 406   | 3                   | 13.67                          | 0.07        |
| 2003             | 393   | 4                   | 10.25                          | 0.10        |
| 1980             | 343   | 5                   | 8.20                           | 0.12        |
| 1997             | 330   | 6                   | 6.83                           | 0.15        |
| 1974             | 317   | 7                   | 5.86                           | 0.17        |
| 1991             | 301   | 8                   | 5.13                           | 0.20        |
| 1999             | 290   | 9                   | 4.56                           | 0.22        |
| 1989             | 287   | 10                  | 4.10                           | 0.24        |
| 2008             | 273   | 11                  | 3.73                           | 0.27        |
| 1986             | 258   | 12                  | 3.42                           | 0.29        |
| 2002             | 257   | 13                  | 3.15                           | 0.32        |
| 1975             | 246   | 14                  | 2.93                           | 0.34        |
| 1978             | 241   | 15                  | 2.73                           | 0.37        |
| 1993             | 233   | 16                  | 2.56                           | 0.39        |
| 1988             | 225   | 17                  | 2.41                           | 0.41        |
| 1987             | 222   | 18                  | 2.28                           | 0.44        |
| 1985             | 212   | 19                  | 2.16                           | 0.46        |
| 2016             | 206   | 20                  | 2.05                           | 0.49        |
| 2011             | 196   | 21                  | 1.95                           | 0.51        |
| 1998             | 194   | 22                  | 1.86                           | 0.54        |
| 1976             | 191   | 23                  | 1.78                           | 0.56        |
| 1982             | 190   | 24                  | 1.71                           | 0.59        |
| 1983             | 187   | 25                  | 1.64                           | 0.61        |
| 1996             | 180   | 26                  | 1.58                           | 0.63        |
| 2012             | 179   | 27                  | 1.52                           | 0.66        |
| 2007             | 174   | 28                  | 1.46                           | 0.68        |
| 2001             | 164   | 29                  | 1.41                           | 0.71        |
| 2010             | 157   | 30                  | 1.37                           | 0.73        |
| 2009             | 156   | 31                  | 1.32                           | 0.76        |
| 1981             | 145   | 32                  | 1.28                           | 0.78        |
| 2004             | 140   | 33                  | 1.24                           | 0.80        |
| 1992             | 139   | 34                  | 1.21                           | 0.83        |
| 2005             | 139   | 35                  | 1.17                           | 0.85        |
| 1994             | 138   | 36                  | 1.14                           | 0.88        |
| 2000             | 137   | 37                  | 1.11                           | 0.90        |
| 1979             | 131   | 38                  | 1.08                           | 0.93        |
| 1977             | 110   | 39                  | 1.05                           | 0.95        |
| 2015             | 99.2  | 40                  | 1.03                           | 0.98        |
|                  |   |                     |                                |             |
| <b>n=</b>        | 40.0  |                     |                                |             |
| <b>mean=</b>     | 234.9   |                     |                                |             |
| <b>Std. Dev=</b> | 114.8   |                     |                                |             |

## Appendix J: Soil Mechanics Calculations

According to (Coduto, Yeung, & Kitch, 2011), “the flow net solution is a graphical method of solving the two-dimensional Laplace Equation.” The theory states that a flow function  $\psi$  and the potential function  $\phi$ , both satisfy this equation and can be constructed to form a grid pattern of equipotential and flow lines. More information on the derivation of this graphical method can be found in Chapter 8, section 2 of Coduto (2011).

The flow net was constructed below in Figure 48 and from the lattice, the pressure head along the base of the concrete slab could be determined. Table 18 below shows the corresponding calculations and the resulting porewater pressure for 11 intervals. This pressure was then added in sectioned intervals and a net uplift force was calculated for a 1m wide section of the structure.

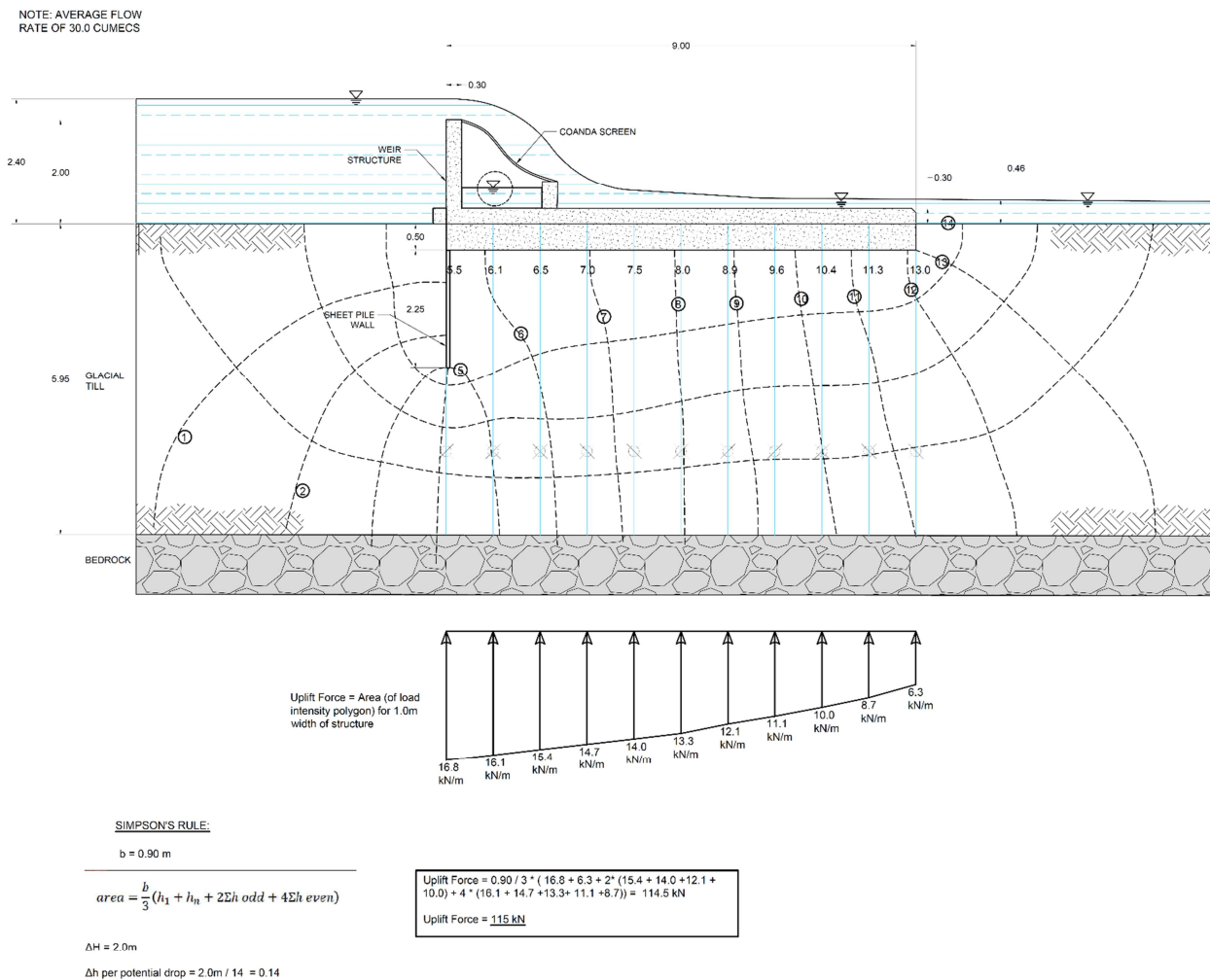


Figure 48 Flow net and uplifting forces



$$w = 22800 \text{ kg} * 9.81 \text{ N/kg} = 223668 \text{ N} = 223.7 \text{ kN}$$

The factor of safety is the weight due to the structure divided by the uplifting force. A value of 1.95 was calculated and is within an acceptable margin.

$$FS = \frac{\text{Resisting force}}{\text{Uplifting force}} = \frac{223.7 \text{ kN}}{114.5 \text{ kN}} = 1.95$$

## Overtuning Moment

Hydrostatic forces will also develop along the backwall of the weir structure, creating a moment about the heel and the toe of the concrete slab. Figure 49 below shows the three resultant forces of primary concern:

- The hydrostatic force (assumed freeboard of 0.4m)
- The uplifting force (due to the porewater pressure)
- The downward force (due to the self-weight of the structure)

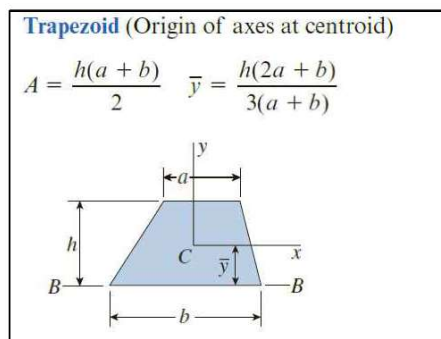
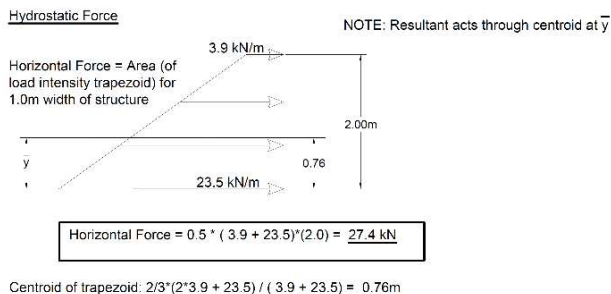
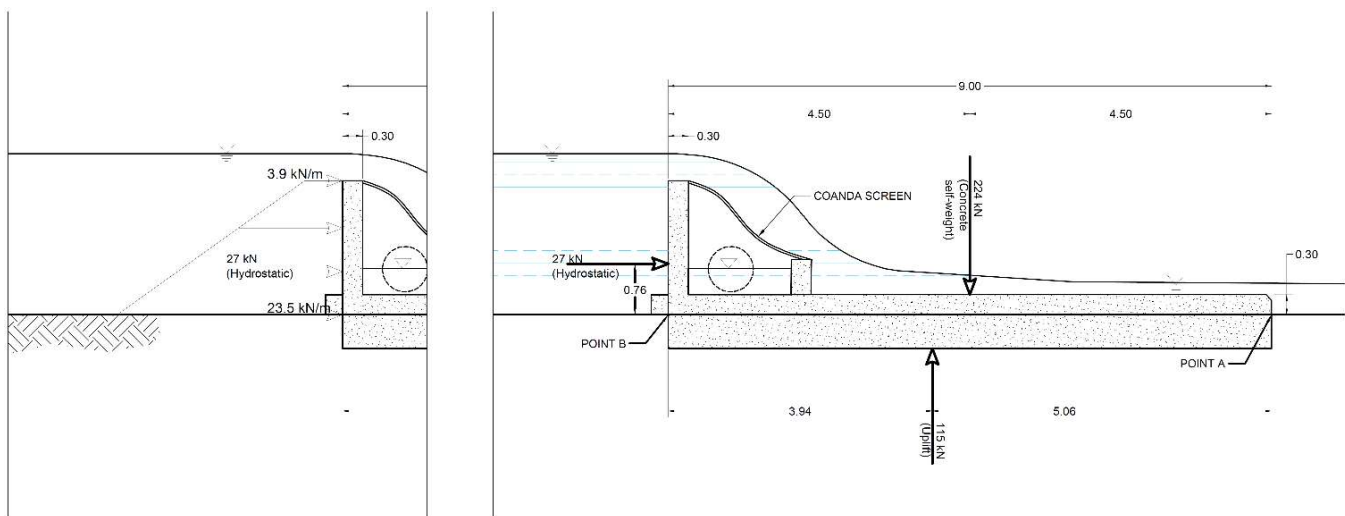


Figure 49 Overtuning moments

The resisting and overturning moments are considered about both point A (the toe) and point B (the heel).

The factor of safety is then given by the sum of all resisting moments divided by the sum of all overturning moments such that:

$$FS = \frac{\sum Moment_{resisting}}{\sum Moment_{overturning}}$$

Considering moments about point A, the factor of safety is given by:

$$FS = \frac{\sum Moment_{resisting}}{\sum Moment_{overturning}} = \frac{224kN * 4.50m}{27kN * 0.76m + 115kN * 5.06m} = 1.67$$

And the moments about point B yield

$$FS = \frac{\sum Moment_{resisting}}{\sum Moment_{overturning}} = \frac{224kN * 4.50m + 27kN * 0.76m}{115kN * 3.94m} = 2.27$$

Both factors of safety calculated above are considered adequate.

## Appendix K: Ogee Profile

The Ogee profile was calculated for a 0.4m freeboard with a design flow of 30.0 cumecs. The accelerator drop plate was designed based on this curve for optimal intake.

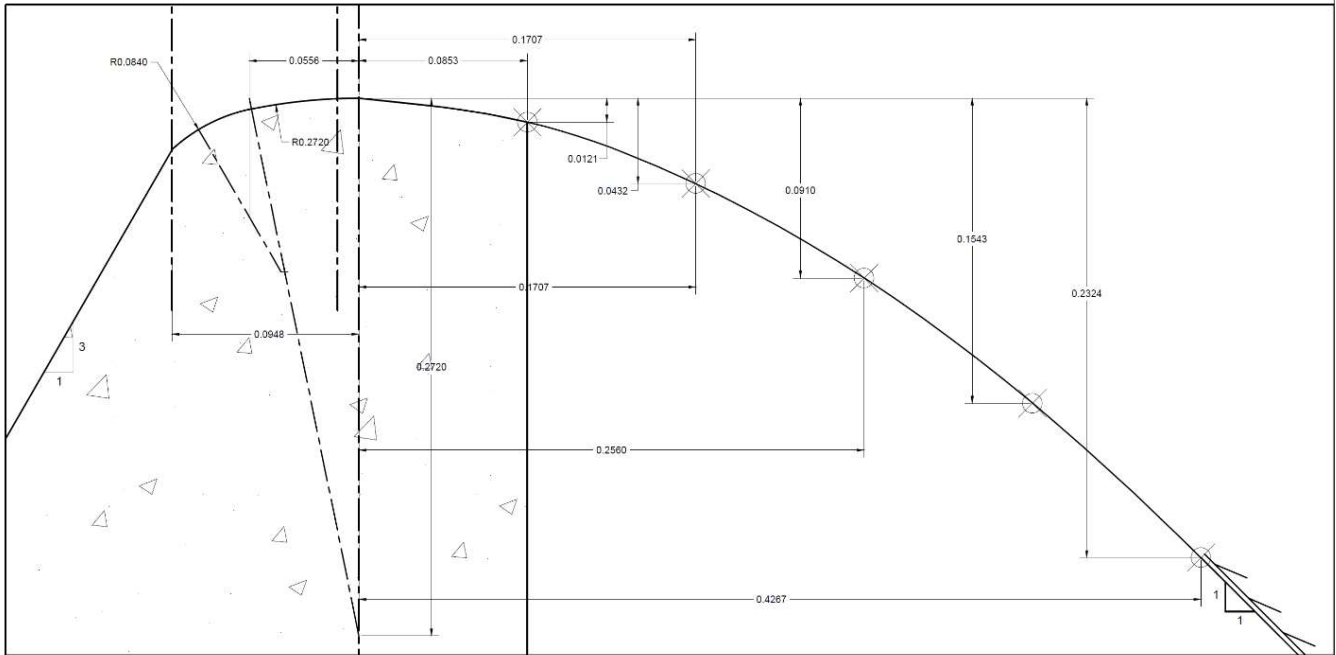


Figure 50 Calculated Ogee profile

## Appendix L: Concrete Weir Structure

The concrete weir structure was drafted using Autocad Revit and is shown below in Figure 51 in several views. The dimensions were based on discharge data taken from the Tulameen River.

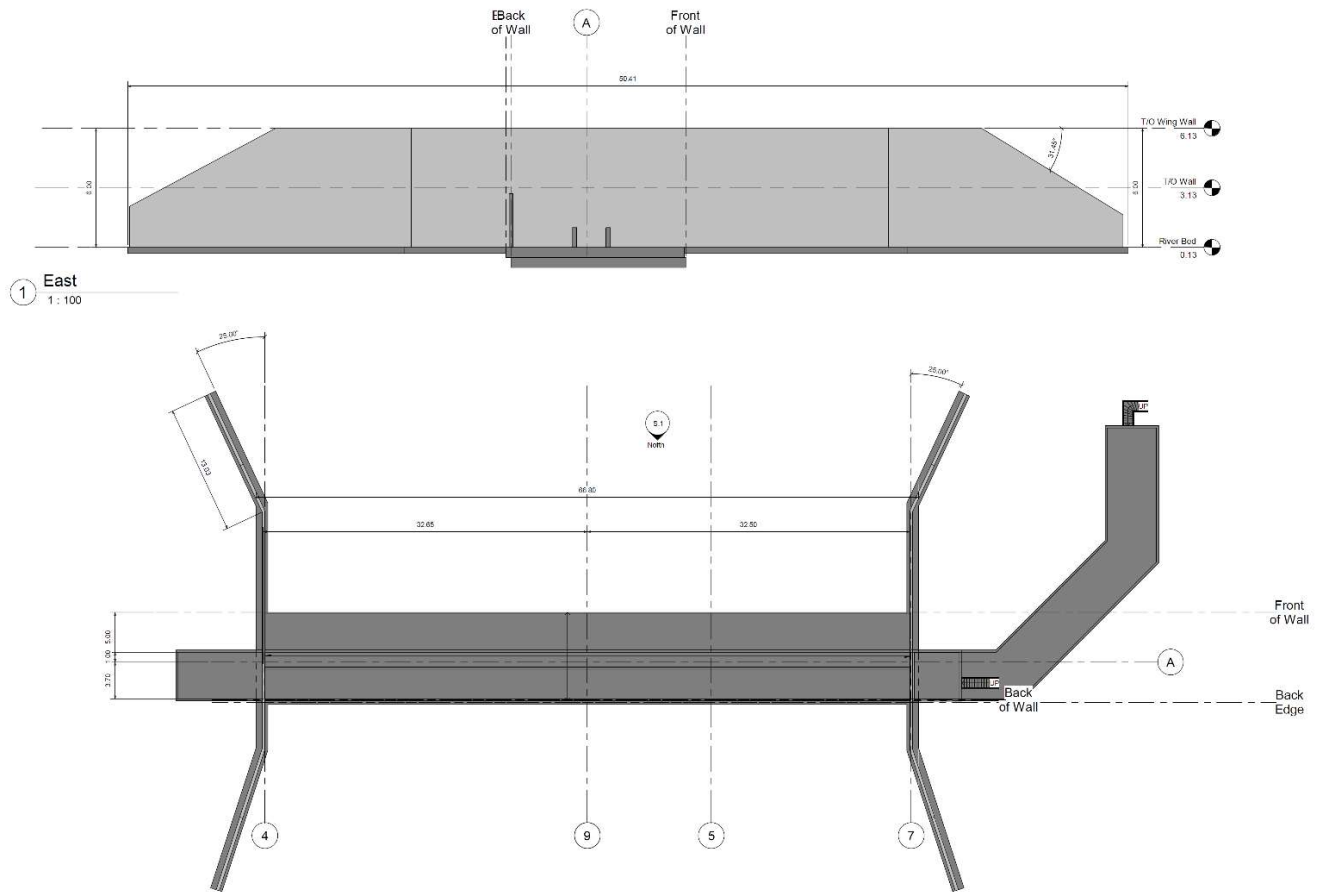


Figure 51 Concrete Weir Structure